UNIVERSITY OF
KWAZULU-NATAL
INYUVESI
YAKWAZULU-NATALI

Experimental investigation of electric-field-induced birefringence in fluids

By

Mzungezi Cyprian Mthembu

Submitted in partial fulfilment of the
requirements for the degree of
Master of Science

in the School of Chemistry and Physics
University of KwaZulu-Natal
November 2014

Contents

List of Figures

Declaration

This dissertation describes the work undertaken at the School of Chemistry and Physics, University of KwaZulu-Natal, Pietermaritzburg Campus under the supervision of Dr V. W. Couling between January 2013 and November 2014.

I declare that the work reported in this dissertation is my own research, unless specifically indicated to the contrary in the text. This dissertation has not been submitted in any form, for any degree or examination to any other university.

Signed: .....

On this ..... day of 2014

I hereby certify that this statement is correct

.....

Dr V. W. Couling

Supervisor

Acknowledgments

I wish to express my sincere gratitude and appreciation to all of the people who have encouraged and assisted me during the course of this work. I would like to express my deepest appreciation to the following people:

My supervisor, Dr V. W. Couling, for his constant guidance and encouragement, and for the time and effort he took in helping me during this work.

The entire Electronics Centre staff, and in particular to Mr G. Dewar, for their tireless assistance in maintaining and repairing the electronic apparatus used in this work.

Mr K. Penzhorn of the Physics Technical Staff for constructing and repairing mechanical components used in the experimental part of this work.

Mr R. Sivraman of the Physics Technical Staff for helping in accessing both tools from the physics workshop, and laboratory equipment required during the project.

Dr S. H. Mthembu for the moral support he gave me.

The National Research Foundation for generous financial support towards my MSc studies.

My family, and especially my mother, for the encouragement and support they gave me during this study.

Abstract

Measurements of the quadratic electro-optical (Kerr) effect of fluids can provide knowledge of fundamental molecular properties, such as (hyper)polarizabilities. They also provide valuable information about intermolecular forces through the measured Kerr-effect virial coefficients. These properties play a considerable role in aspects of physics, chemistry and biology, and so are of inherent value. They also provide benchmarks against which to evaluate *ab inito* quantum mechanical caluclations of the properties, especially for larger atoms and molecules, where the need for large basis sets and adequate account of electron correlation places onerous demands on computational resources.

This thesis reports the development of an apparatus to measure the electric-field-induced birefringence (Kerr effect) in a fluid. The apparatus has been designed in an attempt to increase the precision and absolute accuracy of the measured Kerr effect, with a long-term view to obtaining precise new data for a range of molecular species. The apparatus has been fully automated, using a personal computer containing an IEEE interfacing card to communicate with a data-acquisition and control unit, which in turn controls the experiment and collects the data from which the Kerr constant can be determined.

The apparatus has been used to measure the Kerr constant of gaseous helium at two different temperatures, namely 399.4 K and 445.7 K. Helium was chosen because extremely precise and accurate *ab initio* calculations of this two-electron system have yielded very precise knowledge of the Kerr constant (to within 0.1%), so that it provides an ideal benchmark against which to assess the performance of the apparatus. Once the Kerr apparatus is yielding precise data for helium, it will be possible to measure the Kerr effect of other gaseous species with confidence.

A full Jones calculus analysis of the optical cascade is presented, providing useful insights into the best experimental procedure to be employed in the gathering of data. In addition, the molecular-tensor theory of the second Kerr-effect virial coefficient B_K is reviewed. Measurements of the Kerr-effect of helium gas have yielded the second Kerr hyperpolarizability at the experimental wavelength of 632.8 nm.

Chapter 1

Introduction and Aims

1.1 Introduction and the aims of this work

The experimental and theoretical determination of electromagnetic properties of individual molecules is one of the primary goals of molecular optics. This can be achieved by experimental investigation of how light interacts with macroscopic samples of matter, and then coupling such measurements with suitable molecular-tensor theories to relate the macroscopic observables to the molecular property tensors of the individual molecules in the sample.

Measuring the electro-optical Kerr effect of gases is an important means to determining molecular (hyper)polarizabilities, which provide insight into the structure of molecules. In a typical gas sample, the molecules cannot be treated as though they are independent systems since the presence of molecular interactions affects the bulk properties of the sample, modifying them from that of an ideal gas. The Kerr effect of gases is typically very small in comparison to that of liquids and solids, and so is often extremely difficult to measure with accuracy. This has led to a relative scarcity in experimental data in the case of gases.

This work describes a new apparatus built to undertake precise new measurements of the electro-optic Kerr effect for gases. The accuracy of Kerr-effect measurements depends upon a number of factors, including the path length traversed by the laser beam through the sample to which the electric field has been applied: this Kerr cell has elec-

trodes about 1.5 m in length. A full Jones calculus analysis provides useful insight into the best experimental procedure to be adopted in gathering measured data.

Helium provides a useful standard since the molar Kerr constant is known very precisely from *ab initio* computation. Unfortunately, being a two-electron system, helium has a Kerr constant which is orders of magnitude smaller than that for most other gases, making accurate measurement of the induced birefringence a very challenging task. Once the measurements of helium are in good agreement with the calculated values, it will be possible to turn attention to the measurement of Kerr-effect data for other molecular species.

Chapter 2

Theory of the Kerr Effect

2.1 Introduction

In 1875, Kerr observed that the application of a strong electric field across an isotropic medium results in the medium becoming birefringent [1]. Only gases will be considered in this review: here, the anisotropy induced in the molecular distribution by an applied field arises from both the intrinsic anisotropy of the molecules and the anisotropy induced in the molecules by the applied field. A principal goal of Kerr-effect measurements in gases is the determination of molecular polarizabilities and hyperpolarizabilities, and the Kerr-effect virial coefficients. This requires mathematical relationships between the molecular-property tensors and the macroscopic experimental observables. With the aid of such expressions, molecular-property tensors can be extracted from the measured data. In 1955, Buckingham and Pople developed such a theory for gases comprised of axially-symmetric molecules at low pressures [2]. In 1995, Couling and Graham extended this theory to include gases comprised of molecules with symmetry lower than axial, and included higher-order molecular-interaction terms to ensure convergence to a meaningful result [3, 4]. This theory has been reviewed as part of this MSc project in preparation for calculations when new measured data of molecular species becomes available using our Kerr effect apparatus. This thesis is primarily concerned with calibration of the new apparatus using atomic helium, but the full molecular tensor theory is reviewed here in preparation for future PhD work.

Placing an isotropic gas sample in a strong uniform electric field causes the gas to become

birefringent. This is referred to as the quadratic electro-optic, or Kerr, effect, and the molar Kerr constant ${}_mK$ of a gas is defined as [2]

$$ {}_mK = \frac{6n(n_\parallel - n_\perp)V_m}{(n^2+2)^2(\varepsilon_r+2)^2E^2} \tag{2.1} $$

where n is the isotropic refractive index, ε_r is the dielectric constant of the gas, V_m the molar volume of the gas sample, and $(n_\parallel - n_\perp)$ is the difference in refractive indices for light polarized parallel and perpendicular to the applied electric field E. The virial expansion of the molar Kerr constant is [5]

$$ {}_mK = A_K + \frac{B_K}{V_m} + \frac{C_K}{V_m^2} + \cdots \ , \tag{2.2} $$

where A_K, B_K and C_K are the first, second and third Kerr-effect virial coefficients respectively, and are functions of temperature and optical frequency.

2.2 Non-interacting molecules

Consider a Kerr cell containing an isotropic fluid to which a static electric field is applied. The permanent and induced multipole moments of the molecules will tend to orient themselves to minimize the forces acting on them. The resulting anisotropy results in the medium becoming birefringent. Were a linearly-polarized light beam to pass through this medium, it would emerge elliptically polarized due to the phase difference ϕ induced between the coherent resolved components of the incident beam linearly polarized parallel and perpendicular to the direction of the applied static field. The maximum phase difference ϕ is induced when the angle of azimuth of the linearly polarized incident beam is at $\frac{\pi}{4}$ radians relative to the applied field. For a light beam of wavelength λ which propagates through a birefringent medium of path length l, the induced ϕ is

$$ \phi = \frac{2\pi l(n_\parallel - n_\perp)}{\lambda}. \tag{2.3} $$

If this elliptically-polarized beam is passed through a quarter-wave plate with its fast axis at an azimuth of $\frac{\pi}{4}$, then the light will emerge from it linearly polarized but with its plane of polarization offset from $\frac{\pi}{4}$ by $\frac{\phi}{2}$. The relationship between the Kerr effect and the induced phase difference is given as

$$\phi = 2\pi B l E^2 \tag{2.4}$$

where the Kerr constant B, which can be positive or negative, depends on the particular substance under investigation, its temperature, and the wavelength of the light beam. B is defined as

$$B = \frac{(n_{\parallel} - n_{\perp})}{\lambda E^2}. \tag{2.5}$$

A negative Kerr constant is observed for some polar substances, where the permanent moments of the molecules partially align themselves parallel to the applied electric field.

Consider a Cartesian laboratory frame $O(x, y, z)$ fixed in a Kerr cell such that x and y are parallel and perpendicular, respectively, to the direction of the applied field and z is in the direction of the beam propagating through the cell. For dilute fluids, where molecular interactions are negligible, the induced oscillating dipole moment $\mu_i^{(p)}$ of molecule p will arise only from the oscillating electric field ξ_{0i} of the light beam. Application of a strong static electric field E_i to the fluid modifies the optical-frequency polarizability α_{ij} to a new effective polarizability π_{ij}, written as

$$\pi_{ij} = \frac{\partial \mu_i}{\partial \xi_{0j}} = \alpha_{ij} + \beta_{ijk} E_k + \tfrac{1}{2}\gamma_{ijkl} E_k E_l + \cdots \ , \tag{2.6}$$

where all tensors refer to the molecule-fixed axes $O(1, 2, 3)$ of molecule p. The subscripts i, j denote vector or tensor components, and when a suffix occurs twice in the same term, summation over Cartesian components with respect to that term is understood, as per the Einstein summation convention. The first and second hyperpolarizability tensors β_{ijk}

and γ_{ijkl} describe the distorting effect of the applied field on the polarizability. The first hyperpolarizability is responsible for frequency doubling and the second is responsible for frequency tripling, describing the dipole moments induced by a light wave field that oscillate as twice and three times the incident frequency respectively. Phenomenologically, π_{ij} measures the increase in moment per unit increase in field. In the laboratory frame, the components of the effective polarizability parallel and perpendicular to the direction of the biasing field are

$$\pi_{xx} = l_i^x l_j^x \pi_{ij} \tag{2.7}$$

and

$$\pi_{yy} = l_i^y l_j^y \pi_{ij} \tag{2.8}$$

respectively. Here, l_i^x is the direction cosine between the x space-fixed and the i molecule-fixed axes, while l_i^y is the corresponding direction cosine between the y space-fixed and the i molecule-fixed axes. For a molecule held in a fixed spatial configuration τ, the differential polarizability in the presence of the biasing field is

$$\begin{aligned} \pi(\tau, E) &= \pi_{ij}(l_i^x l_j^x - l_i^y l_j^y) \\ &= (\alpha_{ij} + \beta_{ijk} E l_k^x + \frac{1}{2}\gamma_{ijkl} E^2 l_k^x l_l^x + \cdots)(l_i^x l_j^x - l_i^y l_j^y) \end{aligned} \tag{2.9}$$

where E_i has been written as $E l_i^x$. Since the molecule is tumbling in space, this quantity needs to be averaged over all configurations in the presence of the biasing influence of E_i. At typical experimental temperatures the rotational motion of the molecules can be treated classically. Since the light wave's period of oscillation is much smaller than the time taken for the molecules to rotate, a Boltzmann-type weighting factor can be used to perform the average over molecular configurations:

$$\overline{\pi} = \frac{\int \pi(\tau, E) e^{-U(\tau,E)/k_B T} d\tau}{\int e^{-U(\tau,E)/k_B T} d\tau} \tag{2.10}$$

where $U(\tau, E)$ is the potential energy of the molecule in a specific configuration τ in the

presence of the biasing field. In molecule-fixed axes this is

$$\begin{aligned} U(\tau, E) &= U^0 - \mu_i^{(0)} E_i - \tfrac{1}{2} a_{ij} E_i E_j - \tfrac{1}{6} b_{ijk} E_i E_j E_k + \cdots \\ &= U^0 - \mu_i^{(0)} E l_i^x - \tfrac{1}{2} a_{ij} E^2 l_i^x l_j^x - \tfrac{1}{6} b_{ijk} E^3 l_i^x l_j^x l_k^x + \cdots \end{aligned} \tag{2.11}$$

where the field-free molecular potential energy is U^0, with $\mu_i^{(0)}$ the permanent dipole moment of the molecule, a_{ij} its static polarizability, b_{ijk} its static first order hyperpolarizability, etc. The difference between the refractive indices becomes [2]

$$n_x - n_y = \frac{2\pi N_A}{4\pi\varepsilon_0} \overline{\pi}, \tag{2.12}$$

where N_A is Avogadro's number. The relation between the induced birefringence and the biasing electric field requires evaluation of the average differential polarizability. To achieve this, the biased average can be converted into isotropic averages by Taylor expanding $\bar{\pi}$ in power of E:

$$\overline{\pi} = A + BE + CE^2 + \cdots \,, \tag{2.13}$$

where

$$A = (\overline{\pi})_{E=0} \,,$$

$$B = \left(\frac{\partial \overline{\pi}}{\partial E} \right)_{E=0}$$

and

$$C = \frac{1}{2} \left(\frac{\partial^2 \overline{\pi}}{\partial E^2} \right)_{E=0} .$$

The isotropic average $\langle X \rangle$ of a quantity $X(\tau, E)$ with $E = 0$ is

$$\langle X \rangle = \frac{\int X(\tau, 0) e^{-U^0/k_B T} d\tau}{\int e^{-U^0/k_B T} d\tau}. \tag{2.14}$$

Obtaining expressions for A, B and C requires determination of the isotropic averages of the direction cosines. These general results, quoted by Buckingham and Pople [2] and by Barron [6], are required:

$$\left\{ \begin{array}{c} \langle l_i^x \rangle = \langle l_i^y \rangle = \langle l_i^z \rangle = 0 \\ \\ \langle l_i^x l_j^x \rangle = \langle l_i^y l_j^y \rangle = \langle l_i^z l_j^z \rangle = \frac{1}{3}\delta_{ij} \\ \\ \langle l_i^x l_j^x l_k^x \rangle = \langle l_i^y l_j^y l_k^y \rangle = \langle l_i^z l_j^z l_k^z \rangle = \frac{1}{6}\varepsilon_{ijk} \end{array} \right\} \tag{2.15}$$

and

$$\left\{ \begin{array}{c} \langle l_i^x l_j^x l_k^x l_l^x \rangle = \frac{1}{15}(\delta_{ij}\delta_{kl} + \delta_{ik}\delta_{jl} + \delta_{il}\delta_{kj}) \\ \\ \langle l_i^z l_j^z l_k^x l_l^x \rangle = \frac{1}{30}(4\delta_{ik}\delta_{jl} - \delta_{ij}\delta_{kl} - \delta_{il}\delta_{kj}) \end{array} \right\}. \tag{2.16}$$

When $E = 0$, A becomes zero since $\langle \pi \rangle = 0$: no birefringence is induced in the fluid. Differentiating equation (2.12) with respect to E and putting $E = 0$ yields

$$B = \left(\frac{\partial \overline{\pi}}{\partial E} \right)_{E=0} = \left\langle \frac{\partial \pi}{\partial E} \right\rangle - \frac{1}{k_B T} \left\langle \pi \frac{\partial U}{\partial E} \right\rangle \tag{2.17}$$

where

$$\left\{ \begin{array}{c} \left(\frac{\partial \pi}{\partial E}\right)_{E=0} = \beta_{ijk} l_k^x (l_i^x l_j^x - l_i^y l_j^y) \\ \\ \left(\frac{\partial U}{\partial E}\right)_{E=0} = -\mu_i^{(0)} l_i^x \end{array} \right\}. \tag{2.18}$$

Both of the terms in equation (2.17) average to zero over all directions of l_i^x, the leading non-vanishing term for the differential polarizability being C:

$$C = \frac{1}{2}\left(\frac{\partial^2 \overline{\pi}}{\partial E^2} \right)_{E=0} = \frac{1}{2}\left\langle \frac{\partial^2 \pi}{\partial E^2} \right\rangle - \frac{1}{2k_B T}\left\langle 2\frac{\partial \pi}{\partial E}\frac{\partial U}{\partial E} + \pi \frac{\partial^2 U}{\partial E^2} \right\rangle + \frac{1}{2(k_B T)^2}\left\langle \pi \left(\frac{\partial U}{\partial E} \right)^2 \right\rangle. \tag{2.19}$$

Double-differentiating equations (2.8) and (2.10) and setting the field to zero yields

$$\left\{ \begin{array}{c} \left(\frac{\partial^2 \pi}{\partial E^2}\right)_{E=0} = \gamma_{ijkl} l_k^x l_l^x (l_i^x l_j^x - l_i^y l_j^y) \\ \\ \left(\frac{\partial^2 U}{\partial E^2}\right)_{E=0} = -\alpha_{ij} l_i^x l_j^x \end{array} \right\}. \tag{2.20}$$

Equation (2.15) gives

$$\langle l_i^x l_j^x l_k^x l_l^x - l_i^y l_j^y l_k^x l_l^x \rangle = \tfrac{1}{30}(-2\delta_{ij}\delta_{kl} + 3\delta_{ik}\delta_{jl} + 3\delta_{il}\delta_{jk}) \tag{2.21}$$

so that

$$\left\{ \begin{array}{c} \frac{1}{2}\left\langle \frac{\partial^2 \pi}{\partial E^2} \right\rangle = \tfrac{1}{2}\gamma_{ijkl}\langle l_i^x l_j^x l_k^x l_l^x - l_i^y l_j^y l_k^x l_l^x \rangle \\ \\ = \tfrac{2}{30}\gamma_{iijj}, \end{array} \right\}, \tag{2.22}$$

$$\left\{ \begin{array}{l} -\frac{1}{2k_BT}\langle 2\frac{\partial \pi}{\partial E}\frac{\partial U}{\partial E} + \pi \frac{\partial^2 U}{\partial E^2} \rangle = \frac{1}{k_BT}\beta_{ijk}\mu_l^{(0)}\langle l_i^x l_j^x l_k^x l_l^x - l_i^y l_j^y l_k^x l_l^x \rangle \\ \\ \qquad\qquad + \frac{1}{2k_BT}\alpha_{ij}\alpha_{kl}\langle l_i^x l_j^x l_k^x l_l^x - l_i^y l_j^y l_k^x l_l^x \rangle \\ \\ \qquad\qquad = \frac{2}{15k_BT}\beta_{iij}\mu_j^{(0)} + \frac{1}{15k_BT}(\alpha_{ij}a_{ij} - 3\alpha a), \end{array} \right\}, \tag{2.23}$$

and

$$\left\{ \begin{array}{l} \frac{1}{2(k_BT)^2}\left\langle \pi \left(\frac{\partial U}{\partial E}\right)^2 \right\rangle = \frac{1}{2(k_BT)^2}\alpha_{ij}\mu_k^{(0)}\mu_l^{(0)}\langle l_i^x l_j^x l_k^x l_l^x - l_i^y l_j^y l_k^x l_l^x \rangle \\ \\ \qquad\qquad = \frac{3}{15(k_BT)^2}(\alpha_{ij}\mu_i^{(0)}\mu_j^{(0)} - \alpha(\mu^{(0)})^2), \end{array} \right\}, \tag{2.24}$$

where $\alpha = \alpha_{ii}$ and $a = a_{ii}$. Thus

$$\tfrac{1}{2}\left(\tfrac{\partial^2\overline{\pi}}{\partial E^2}\right)_{E=0} = \tfrac{2}{30}\gamma_{iijj} + \tfrac{2}{15k_BT}\beta_{iij}\mu_j^{(0)} + \tfrac{1}{15k_BT}(\alpha_{ij}a_{ij} - 3\alpha a) + \tfrac{3}{15(k_BT)^2}(\alpha_{ij}\mu_i^{(0)}\mu_j^{(0)} - \alpha(\mu^{(0)})^2), \quad (2.25)$$

and equation (2.12) becomes

$$\overline{\pi} = \left\{\tfrac{2}{30}\gamma_{iijj} + \tfrac{2}{15k_BT}\beta_{iij}\mu_j^{(0)} + \tfrac{1}{15k_BT}(\alpha_{ij}a_{ij} - 3\alpha a) + \tfrac{3}{15(k_BT)^2}(\alpha_{ij}\mu_i^{(0)}\mu_j^{(0)} - \alpha(\mu^{(0)})^2)\right\} E^2. \quad (2.26)$$

Here the mean dynamic and static polarizabilities are

$$\left\{\begin{array}{l} \alpha = \tfrac{1}{3}(\alpha_{11} + \alpha_{22} + \alpha_{33}) \\ \\ a = \tfrac{1}{3}(a_{11} + a_{22} + a_{33}) \end{array}\right\}. \quad (2.27)$$

In the limit of low density, the definition of the Kerr constant proposed by Otterbein [7] becomes

$${}_mK = \lim_{V_m\to\infty}\left\{\frac{2(n_x - n_y)V_m}{27(4\pi\varepsilon_0)E^2}\right\}_{E=0} = \frac{2\pi N_A}{27(4\pi\varepsilon_0)}\left(\frac{\partial^2\overline{\pi}}{\partial E^2}\right)_{E=0}. \quad (2.28)$$

Invoking equations (2.25), (2.11) and (2.1) yields

$${}_mK = \tfrac{2\pi N_A}{405(4\pi\varepsilon_0)}\left\{2\gamma_{iijj} + \tfrac{1}{k_BT}\left[4\beta_{iij}\mu_j^{(0)} + 2(\alpha_{ij}a_{ij} - 3\alpha a)\right] + \tfrac{6}{(k_BT)^2}\left(\alpha_{ij}\mu_i^{(0)}\mu_j^{(0)} - \alpha(\mu^{(0)})^2\right)\right\}. \quad (2.29)$$

This equation is a generalization of the Langevin-Born equation to take into account the effect of high field strengths on the polarizability. This general expression becomes greatly simplified for molecules of high symmetry.

The temperature-independent contribution to the Kerr effect, which is proportional to the second hyperpolarizability, accounts for a measurable Kerr constant for atomic gases

like the helium used in this project, as well as for isotropically polarizable molecules such as methane. The Langevin-Born theory predicts a zero effect for such systems, while in fact the molar Kerr constant is

$$ {}_mK = \frac{4\pi N_A}{81(4\pi\varepsilon_0)}\gamma^K. \tag{2.30} $$

Here, γ^K is the second Kerr hyperpolarizability, defined by [2]

$$ \gamma^K = \frac{1}{10}(3\gamma_{ijij} - \gamma_{iijj}). \tag{2.31} $$

2.3 Interacting molecules

This Langevin-Born and Buckingham-Pople theory of electro-optical birefringence for assemblies of non-interacting molecules needs modification if it is to account for a dense fluid where intermolecular interactions are present. The molar Kerr constant becomes, as per equation (2.2),

$$ {}_mK = A_K + \frac{B_K}{V_m} + \frac{C_K}{V_m^2} + \cdots , \tag{2.32} $$

where the coefficients A_K, B_K and C_K are the first, second and third Kerr virial coefficients, describing the contributions to the molar Kerr constant arising from non-interacting molecules, interacting pairs of molecules and interacting triplets respectively. The low-density molar Kerr constant A_K is

$$ A_K = \lim_{V_m\to\infty}({}_mK). $$

B_K describes the contribution to ${}_mK$ from interacting pairs of molecules:

$$ B_K = \lim_{V_m\to\infty}({}_mK - A_K)V_m. \tag{2.33} $$

Buckingham presented a statistical-mechanical theory of B_K for axially-symmetric molecules in 1955 [5]. Buckingham and Orr extended this theory in 1969, including additional effects of polarizability and angle-dependent repulsive forces, calculating values of B_K for CH_2F_2, CH_3F and CHF_3 [8]. Approximate agreement with their experimental values for CH_3F was obtained, but the calculated values for CHF_3 were found to be far too small [8]. They attributed this to effects of short-range interactions on the polarizability and potential energy, arguing that measurements of B_K for polar gases probably wouldn't yield useful information about the nature of intermolecular forces. In 1983, Buckingham *et al.* resolved this conflict between experiment and theory for the fluoromethanes [9]. The theory of B_K was extended to include the collision-induced polarizability, which was in fact the dominant contributor to B_K. A simple Stockmayer-type potential yielded a reasonable fit to the measured data for the fluoromethanes over a range of temperature. A limiting factor is the large uncertainty of around 50% in the experimental values. In 1988, Couling and Graham developed a complete molecular-tensor theory of B_K for interacting molecules of general symmetry [3, 4]. This theory has been reviewed in this project in preparation for the measurement of more precise B_K data for molecular species, which is an aim of future PhD work with the existing Kerr-effect apparatus. The present experimental work has focused on the atomic species of helium as a means of accurately characterizing the Kerr-effect apparatus developed here. Helium is a good benchmark for characterizing the experimental apparatus since its hyperpolarizability tensor, and hence its molar Kerr constant, can be computed by *ab initio* quantum mechanical techniques to a high degree of accuracy of around 0.1%. Unfortunately, this Kerr constant is particularly tiny, making its precise and accurate measurement an extremely challenging undertaking. Once this characterization is complete, the apparatus can be used with confidence in measuring the Kerr effect of other molecular species.

As already shown, for an ideal gas, the molecular theory of the Kerr effect has the refractive index difference (n_x - n_y) in the presence of a strong static electric field E_x of

$$n_x - n_y = \frac{2\pi N_A}{(4\pi\varepsilon_0)V_m}\overline{\pi} \tag{2.34}$$

where $\overline{\pi}$ is the average over all configurations of $\pi_{ij}(l_i^x l_j^x - l_i^y l_j^y)$ of a representative isolated molecule in the presence of the biasing influenced E_x.

At higher gas pressures, the representative molecule 1's contribution to (n_x - n_y) is modified by a neighbouring molecule 2. For a pair of interacting molecules in a specified relative configuration τ, the contribution of molecule 1 to the induced birefringence at that particular moment in time will be half of the total contribution of the interacting pair:

$$\frac{1}{2}\left\{\frac{2\pi N_A}{(4\pi\varepsilon_0)V_m}\pi^{(12)}(\tau,E)\right\}. \tag{2.35}$$

Here,

$$\pi^{(12)}(\tau,E) = \pi_{ij}^{(12)}(l_i^x l_j^x - l_i^y l_j^y) \tag{2.36}$$

where $\pi_{ij}^{(12)}$ is the differential polarizability of the interacting pair in molecule-fixed axes. At first, the two molecules which comprise the interacting pair are treated as held in a fixed relative configuration τ, and are allowed to rotate as rigid whole in the presence of the biasing electric field E_i. This yields a biased orientational average $\overline{\pi^{(12)}(\tau,E)}$ which can subsequently be converted into isotropic averages by Taylor expansion in powers of E. Unsurprisingly, the leading surviving term is in E^2:

$$\overline{\pi^{(12)}(\tau,E)} = \frac{1}{2}\left(\frac{\partial^2\overline{\pi^{(12)}(\tau,E)}}{\partial E^2}\right)_{E=0} E^2 \tag{2.37}$$

where

$$\begin{aligned}\frac{1}{2}\left(\frac{\partial^2\overline{\pi^{(12)}(\tau,E)}}{\partial E^2}\right)_{E=0} =& \frac{1}{2}\left\langle\frac{\partial^2\pi^{(12)}}{\partial E^2}\right\rangle - \frac{1}{2k_BT}\left\langle 2\frac{\partial\pi^{(12)}}{\partial E}\frac{\partial U^{(12)}}{\partial E} + \pi^{(12)}\frac{\partial^2 U^{(12)}}{\partial E^2}\right\rangle \\ &+ \frac{1}{2(k_BT)^2}\left\langle\pi^{(12)}\left(\frac{\partial U^{(12)}}{\partial E}\right)^2\right\rangle.\end{aligned} \tag{2.38}$$

Here, $U^{(12)}(\tau, E)$ is the potential energy of the interacting pair of molecules in the presence of E_i. The ideal-gas definition of the molecular Kerr constant proposed by Otterbein was provided in equation (2.27). The molar Kerr constant at higher densities becomes

$$ {}_mK = A_K + \int_\tau \frac{2\pi N_A}{27(4\pi\varepsilon_0)} \left\{ \frac{1}{2} \left(\frac{\partial^2 \overline{\pi^{(12)}(\tau, E)}}{\partial E^2} \right)_{E=0} - \left(\frac{\partial^2 \overline{\pi}}{\partial E^2} \right)_{E=0} \right\} P(\tau) d\tau \qquad (2.39) $$

where $P(\tau)d\tau$ is the probability of molecule 1 having a neighbour in the range (τ, τ + $d\tau$). This probability is related to the intermolecular potential $U^{(12)}(\tau)$ through

$$ P(\tau) = \frac{N_A}{\Omega V_m} e^{-(U^{(12)}(\tau)/k_B T)} \qquad (2.40) $$

where $\Omega = V_m^{-1} \int d\tau$ is the integral over the orientational coordinates of the neighbouring molecule 2. Comparing equations (2.30) and (2.37), the second Kerr virial coefficient can be written as

$$ B_K = \frac{2\pi N_A^2}{27\Omega(4\pi\varepsilon_0)} \int_\tau \left\{ \frac{1}{2} \left(\frac{\partial^2 \overline{\pi^{(12)}(\tau, E)}}{\partial E^2} \right)_{E=0} - \left(\frac{\partial^2 \overline{\pi}}{\partial E^2} \right)_{E=0} \right\} e^{-(U^{(12)}(\tau)/k_B T)} d\tau. \qquad (2.41) $$

In the general case of molecules of symmetry lower than axial, the interaction coordinates are best expressed by the Euler angles and the intermolecular displacement by R (as detailed in Appendix A.1), so that B_K can be written as

$$ B_K = \frac{N_A^2}{216\pi^2(4\pi\varepsilon_0)} \int_{R=0}^{\infty} \int_{\alpha_1=0}^{2\pi} \int_{\beta_1=0}^{\pi} \int_{\gamma_1=0}^{2\pi} \int_{\alpha_2=0}^{2\pi} \int_{\beta_2=0}^{\pi} \int_{\gamma_2=0}^{2\pi} $$

$$ \times \left\{ \frac{1}{2} \left(\frac{\partial^2 \overline{\pi^{(12)}(\tau, E)}}{\partial E^2} \right)_{E=0} - \left(\frac{\partial^2 \overline{\pi}}{\partial E^2} \right)_{E=0} \right\} e^{-(U^{(12)}(\tau)/k_B T)} \qquad (2.42) $$

$$ \times R^2 sin\beta_1 sin\beta_2 dR d\alpha_1 d\beta_1 d\gamma_1 d\alpha_2 d\beta_2 d\gamma_2. $$

Just as in the case of an ideal gas, the refractive index of a dense gas is determined by the total oscillating dipole moment induced in a molecule. However, the dipole moment

of a representative molecule 1 is now induced both by the oscillating electric field ξ_{0i} associated with the light wave, and also partly by the field $F_i^{(1)}$ at molecule 1 arising from the oscillating moments of the neighbouring molecule 2. The dipole moment of molecule 1 becomes

$$\mu_i^{(1)}(\xi_0) = (\alpha_{ij}^{(1)} + \beta_{ijk}^{(1)} E_k + \tfrac{1}{2}\gamma_{ijkl}^{(1)} E_k E_l + ...)(\xi_{0j} + F_j^{(1)}) \tag{2.43}$$

where E_i is the strong applied static field. The quadrupole and field-gradient effects are small enough that their contributions can be safely omitted. The relation between the dipole moment of molecule 2 and the field due to this oscillating moment measured at the origin of molecule 1 is expressed via a $T-$tensor (see Appendix A.1) as

$$F_i^{(1)} = T_{ij}^{(1)} \mu_j^{(2)}. \tag{2.44}$$

The dipole moment of molecule 2 is itself modified by molecule 1's oscillating dipole moment together with the field of the light beam:

$$\mu_i^{(2)}(\xi_0) = (\alpha_{ij}^{(2)} + \beta_{ijk}^{(2)} E_k + \tfrac{1}{2}\gamma_{ijkl}^{(2)} E_k E_l + ...)(\xi_{0j} + F_j^{(2)}). \tag{2.45}$$

The electric field arising at the origin of molecule 2 from the oscillating dipole moment of molecule 1 is

$$F_i^{(2)} = T_{ij}^{(2)} \mu_j^{(1)}. \tag{2.46}$$

Ultimately, the expression for the total dipole of molecule 1 is achieved by substituting equations (2.43) and (2.44) into equation (2.42), followed by successive substitutions of $F_i^{(1)}$ and $F_i^{(2)}$. A lengthy series of terms contributing to the net field $F_i^{(1)}$ in equation (2.42) arises. Substituting this series into equation (2.41) yields the final expression for the total oscillating dipole induced on molecule 1 by the light wave field in the presence of molecule 2. This (lengthy) expression is presented in Appendix A.2. Differentiating this expression with respect to ξ_{0i} yields the differential polarizability of a general molecule p

in the presence of both the static applied field E_i and a neighbouring molecule q, which is also presented in Appendix A.2.

The difference between the differential polarizabilities $\pi_{ij}^{(p)} l_i^x l_j^x$ and $\pi_{ij}^{(p)} l_i^y l_j^y$ for a specific relative interaction configuration τ of molecules p and q in the presence of the applied field is

$$\pi^{(p)}(\tau, E) = \pi_{ij}^{(p)}(l_i^x l_j^x - l_i^y l_j^y). \tag{2.47}$$

It is necessary to assume that the interacting molecules each retain their separate identities, an assumption which is valid in the long-range limit. When the molecules come close together so that their charge distributions begin to overlap, *ab initio* quantum calculations are required, and these are beyond the scope of this analysis. Treating the interacting molecules as if they retain their separate identities even in the overlap region, the total dipole of the interacting pair is

$$\mu_i^{(12)} = \mu_i^{(1)} + \mu_i^{(2)} \tag{2.48}$$

which allows the differential polarizability of the interacting pair to be written as

$$\pi_{ij}^{(12)} = \frac{\partial \mu_i^{(12)}}{\partial \xi_{0j}} = \frac{\partial(\mu_i^{(1)} + \mu_i^{(2)})}{\partial \xi_{0j}}. \tag{2.49}$$

The difference between the differential polarizabilities $\pi_{ij}^{(12)} l_i^x l_j^x$ and $\pi_{ij}^{(12)} l_i^y l_j^y$ of an interacting pair in a specific relative interaction configuration τ in the presence of the applied field becomes

$$\begin{aligned} \pi^{(12)}(\tau, E) &= \pi_{ij}^{(12)}(l_i^x l_j^x - l_i^y l_j^y) \\ &= (\pi_{ij}^{(1)} + \pi_{ij}^{(2)})(l_i^x l_j^x - l_i^y l_j^y) \\ &= \pi^{(1)}(\tau, E) + \pi^{(2)}(\tau, E). \end{aligned} \tag{2.50}$$

The potential energy of the interacting pair in the presence of the biasing electric field is

$$U^{(12)}(\tau, E) = U^{(12)}(\tau, 0) - \int_0^E \mu_i^{(12)}(\tau, E) l_i^x dE \tag{2.51}$$

where E_i has been written as $E\, l_i^x$ and $\mu_i^{(12)}$ is the total dipole moment of the pair in the presence of E_i.

The dipole moment of molecule p in the presence of another molecule q and E_i can be written as

$$\mu_i^{(p)} = \mu_{0i}^{(p)} + a_{ij}^{(p)}(E_j + F_j^{(p)}) \tag{2.52}$$

where $F_i^{(p)}$ is the static field at molecule p due to the permanent and induced multipole moments of molecule q, and $\mu_{0i}^{(p)}$ is the permanent dipole moment of molecule p. This field is related to the inducing dipole moment with the aid of a $T-$tensor:

$$F_i^{(p)} = T_{ij}\mu_j^{(q)}. \tag{2.53}$$

The total dipole moment of molecule q is

$$\mu_i^{(q)} = \mu_{0i}^{(q)} + a_{ij}^{(q)}(E_j + F_j^{(q)}) \tag{2.54}$$

where

$$F_j^{(q)} = T_{ij}\mu_j^{(p)}. \tag{2.55}$$

As before (with the total oscillating dipole moment), successive substitutions are carried out, yielding the series of terms which contribute to the total static dipole moment of

molecule p. The potential energy of the interacting pair becomes

$$U^{(12)}(\tau, E) = U^{(12)}(\tau, 0) + U^{(1)}(\tau, E) + U^{(2)}(\tau, E). \tag{2.56}$$

The explicit expression for the potential energy of molecule p is presented in Appendix A.3. The term $\frac{1}{2}\left(\frac{\partial^2\overline{\pi^{(12)}(\tau,E)}}{\partial E^2}\right)_{E=0}$ in the expression for B_K given by equation (2.39) can now be evaluated. The isotropic averages in equation (2.36), namely

$$\begin{aligned}\frac{1}{2}\left(\frac{\partial^2\overline{\pi^{(12)}(\tau,E)}}{\partial E^2}\right)_{E=0} =& \frac{1}{2}\left\langle\frac{\partial^2\pi^{(12)}}{\partial E^2}\right\rangle - \frac{1}{2k_BT}\left\langle 2\frac{\partial\pi^{(12)}}{\partial E}\frac{\partial U^{12}}{\partial E} + \pi^{12}\frac{\partial^2 U^{12}}{\partial E^2}\right\rangle \\ &+ \frac{1}{2(k_BT)^2}\left\langle\pi^{(12)}\left(\frac{\partial U^{(12)}}{\partial E}\right)^2\right\rangle,\end{aligned} \tag{2.57}$$

are now evaluated. Equation (2.48) coupled with the recognition that molecules 1 and 2 are identical, so that the isotropic averages of their polarizabilities must be the same, allows for the following rearrangement:

$$\begin{aligned}\frac{1}{2}\left\langle\frac{\partial^2\pi^{(12)}}{\partial E^2}\right\rangle &= \frac{1}{2}\left\langle\frac{\partial^2\pi^{(1)}}{\partial E^2}\right\rangle + \frac{1}{2}\left\langle\frac{\partial^2\pi^{(2)}}{\partial E^2}\right\rangle \\ &= \left\langle\frac{\partial^2\pi^{(1)}}{\partial E^2}\right\rangle.\end{aligned} \tag{2.58}$$

Similar arguments, together with equation (2.54), yields

$$\left\{\begin{array}{l}\left\langle\dfrac{\partial\pi^{(12)}}{\partial E}\dfrac{\partial U^{(12)}}{\partial E}\right\rangle = \left\langle 2\dfrac{\partial\pi^{(1)}}{\partial E}\dfrac{\partial U^{(1)}}{\partial E}\right\rangle + \left\langle 2\dfrac{\partial\pi^{(1)}}{\partial E}\dfrac{\partial U^{(2)}}{\partial E}\right\rangle \\ \\ \left\langle\pi^{(12)}\dfrac{\partial^2 U^{(12)}}{\partial E^2}\right\rangle = \left\langle 2\pi^{(1)}\dfrac{\partial^2 U^{(1)}}{\partial E^2}\right\rangle + \left\langle 2\pi^{(1)}\dfrac{\partial^2 U^{(2)}}{\partial E^2}\right\rangle\end{array}\right\} \tag{2.59}$$

and

$$\left\langle\pi^{(12)}\left(\frac{\partial U^{(12)}}{\partial E}\right)^2\right\rangle = 2\left[\left\langle\pi^{(1)}\left(\frac{\partial U^{(1)}}{\partial E}\right)^2\right\rangle + \left\langle 2\pi^{(1)}\frac{\partial U^{(1)}}{\partial E}\frac{\partial U^{(2)}}{\partial E}\right\rangle + \left\langle\pi^{(1)}\left(\frac{\partial U^{(2)}}{\partial E}\right)^2\right\rangle\right]. \tag{2.60}$$

Collecting the expressions gives

$$\frac{1}{2}\left(\frac{\partial^2\overline{\pi^{(12)}(\tau,E)}}{\partial E^2}\right)_{E=0} = \left\langle\frac{\partial^2\pi^{(1)}}{\partial E^2}\right\rangle - \frac{1}{k_BT}\left\{\left\langle 2\frac{\partial\pi^{(1)}}{\partial E}\frac{\partial U^{(1)}}{\partial E}\right\rangle + \left\langle 2\frac{\partial\pi^{(1)}}{\partial E}\frac{\partial U^{(2)}}{\partial E}\right\rangle\right\}$$

$$- \frac{1}{k_BT}\left\{\left\langle \pi^{(1)}\frac{\partial^2 U^{(1)}}{\partial E^2}\right\rangle + \left\langle \pi^{(1)}\frac{\partial^2 U^{(2)}}{\partial E^2}\right\rangle\right\}$$

$$+ \frac{1}{(k_BT)^2}\left\{\left\langle \pi^{(1)}\left(\frac{\partial U^{(1)}}{\partial E}\right)^2\right\rangle + \left\langle \pi^{(1)}\left(\frac{\partial U^{(2)}}{\partial E}\right)^2\right\rangle\right\}$$

$$+ \frac{1}{(k_BT)^2}\left\langle 2\pi^{(1)}\frac{\partial U^{(1)}}{\partial E}\frac{\partial U^{(2)}}{\partial E}\right\rangle. \tag{2.61}$$

It becomes possible to write

$$\left\{\frac{1}{2}\left(\frac{\partial^2\overline{\pi^{(12)}(\tau,E)}}{\partial E^2}\right)_{E=0} - \left(\frac{\partial^2\overline{\pi}}{\partial E^2}\right)_{E=0}\right\} = \alpha_2+\alpha_3+\alpha_4+\alpha_5+\cdots+\gamma_1\alpha_1+\gamma_1\alpha_2+\cdots$$

$$+\mu_2\alpha_1+\mu_2\alpha_2+\mu_2\alpha_3+\cdots+\mu_1\beta_1+\mu_1\beta_1\alpha_1+\cdots, \tag{2.62}$$

where

$$\alpha_2 = \frac{1}{k_BT}\left\{\alpha_{ij}^{(1)}a_{kl}^{(2)}\right\}\left\langle l_i^x l_j^x l_k^x l_l^x - l_i^y l_j^y l_k^y l_l^y\right\rangle, \tag{2.63}$$

$$\alpha_3 = \frac{1}{k_BT}\left\{\alpha_{ij}^{(1)}a_{km}^{(2)}T_{mn}a_{nr}^{(2)} + \alpha_{ij}^{(1)}a_{km}^{(2)}T_{mn}a_{nr}^{(1)} + \alpha_{im}^{(1)}T_{mn}\alpha_{nj}^{(2)}a_{kr}^{(1)} + \alpha_{im}^{(1)}T_{mn}\alpha_{nj}^{(2)}a_{kr}^{(2)}\right\}$$

$$\times\left\langle l_i^x l_j^x l_k^x l_r^x - l_i^y l_j^y l_k^y l_l^y\right\rangle, \tag{2.64}$$

$$\alpha_4 = \frac{1}{k_B T}\Big\{ \alpha^{(1)}_{ij} a^{(1)}_{kl} T_{lm} a^{(2)}_{mw} T_{wv} a^{(1)}_{vr} + \alpha^{(1)}_{ij} a^{(2)}_{kl} T_{lm} a^{(1)}_{mw} T_{wv} a^{(2)}_{vr} +$$

$$\alpha^{(1)}_{im} T_{mn} \alpha^{(2)}_{nj} a^{(1)}_{kw} T_{wv} a^{(2)}_{vr} + \alpha^{(1)}_{im} T_{mn} \alpha^{(2)}_{nj} a^{(2)}_{kw} T_{wv} a^{(1)}_{vr} +$$

$$\alpha^{(1)}_{im} T_{mn} \alpha^{(2)}_{nw} T_{wv} \alpha^{(1)}_{vj} a^{(1)}_{kr} + \alpha^{(1)}_{im} T_{mn} \alpha^{(2)}_{nw} T_{wv} \alpha^{(1)}_{vj} a^{(2)}_{kr} \Big\} \left\langle l^x_i l^x_j l^x_k l^x_r - l^y_i l^y_j l^y_k l^y_l \right\rangle , \quad (2.65)$$

$$\alpha_5 = \frac{1}{k_B T}\Big\{ \alpha^{(1)}_{ij} a^{(1)}_{kl} T_{lm} a^{(2)}_{mn} T_{nw} a^{(1)}_{wv} T_{vu} a^{(2)}_{ur} + \alpha^{(1)}_{ij} a^{(2)}_{kl} T_{lm} a^{(1)}_{mn} T_{nw} a^{(2)}_{wv} T_{vu} a^{(1)}_{ur}$$

$$+ \alpha^{(1)}_{ij} T_{kl} \alpha^{(2)}_{lm} a^{(1)}_{mn} T_{nw} a^{(2)}_{wv} T_{vu} a^{(1)}_{ur} + \alpha^{(1)}_{ij} T_{kl} \alpha^{(2)}_{lm} a^{(2)}_{mn} T_{nw} a^{(1)}_{wv} T_{vu} a^{(2)}_{ur}$$

$$+ \alpha^{(1)}_{ij} T_{kl} \alpha^{(2)}_{lm} T_{mn} \alpha^{(1)}_{nw} a^{(1)}_{wv} T_{vu} a^{(2)}_{ur} + \alpha^{(1)}_{ij} T_{kl} \alpha^{(2)}_{lm} T_{mn} \alpha^{(1)}_{nw} a^{(2)}_{wv} T_{vu} a^{(1)}_{ur}$$

$$+ \alpha^{(1)}_{ij} T_{kl} \alpha^{(2)}_{lm} T_{mn} \alpha^{(1)}_{nw} T_{wv} \alpha^{(2)}_{vu} a^{(1)}_{ur} + \alpha^{(1)}_{ij} T_{kl} \alpha^{(2)}_{lm} T_{mn} \alpha^{(1)}_{nw} T_{wv} \alpha^{(2)}_{vu} a^{(2)}_{ur} \Big\}$$

$$\times \left\langle l^x_i l^x_j l^x_k l^x_r - l^y_i l^y_j l^y_k l^y_r \right\rangle , \quad (2.66)$$

$$\gamma_1 \alpha_1 = \left\{ \gamma^{(1)}_{ijkl} T_{lw} \alpha^{(2)}_{wr} + \alpha^{(1)}_{iw} T_{wl} \gamma^{(2)}_{ljkr} \right\} \left\langle l^x_i l^x_j l^x_k l^x_r - l^y_i l^y_j l^y_k l^y_r \right\rangle , \quad (2.67)$$

$$\mu_2 \alpha_1 = \frac{1}{(k_B T)^2} \left\{ \alpha^{(1)}_{ij} \mu^{(2)}_{0k} \mu^{(2)}_{0r} + 2\alpha^{(1)}_{ij} \mu^{(1)}_{0k} \mu^{(2)}_{0r} \right\} \left\langle l^x_i l^x_j l^x_k l^x_r - l^y_i l^y_j l^y_k l^y_r \right\rangle , \quad (2.68)$$

$$\mu_2\alpha_2 = \frac{1}{(k_BT)^2}\Big\{2\alpha^{(1)}_{ij}\mu^{(1)}_{0k}a^{(1)}_{rm}T_{mn}\mu^{(2)}_{0n} + 2\alpha^{(1)}_{ij}\mu^{(2)}_{0k}a^{(2)}_{rm}T_{mn}\mu^{(1)}_{0n}$$

$$+ 2\alpha^{(1)}_{ij}\mu^{(1)}_{0k}a^{(2)}_{rm}T_{mn}\mu^{(1)}_{0n} + 2\alpha^{(1)}_{ij}\mu^{(2)}_{0k}a^{(1)}_{rm}T_{mn}\mu^{(2)}_{0n}$$

$$+ \alpha^{(1)}_{im}T_{mn}\alpha^{(2)}_{nj}\mu^{(1)}_{0k}\mu^{(1)}_{0r} + \alpha^{(1)}_{im}T_{mn}\alpha^{(2)}_{nj}\mu^{(2)}_{0k}\mu^{(2)}_{0r}$$

$$+ 2\alpha^{(1)}_{im}T_{mn}\alpha^{(2)}_{nj}\mu^{(1)}_{0k}\mu^{(2)}_{0r}\Big\}\left\langle l^x_i l^x_j l^x_k l^x_r - l^y_i l^y_j l^y_k l^y_r\right\rangle, \tag{2.69}$$

$$\mu_2\alpha_3 = \frac{1}{k_BT}\Big\{\alpha^{(1)}_{ij}\alpha^{(1)}_{kl}T_{lm}\mu^{(2)}_{0m}a^{(1)}_{rn}T_{nw}\mu^{(2)}_{0w} + \alpha^{(1)}_{ij}\alpha^{(2)}_{kl}T_{lm}\mu^{(1)}_{0m}a^{(2)}_{rn}T_{nw}\mu^{(1)}_{0w}$$

$$+ 2\alpha^{(1)}_{ij}\alpha^{(1)}_{kl}T_{lm}\mu^{(2)}_{0m}a^{(2)}_{rn}T_{nw}\mu^{(1)}_{0w} + 2\alpha^{(1)}_{im}T_{mn}\alpha^{(2)}_{nj}\mu^{(1)}_{0k}a^{(1)}_{rw}T_{wv}\mu^{(2)}_{0v}$$

$$+ 2\alpha^{(1)}_{im}T_{mn}\alpha^{(2)}_{nj}\mu^{(2)}_{0k}a^{(2)}_{rw}T_{wv}\mu^{(1)}_{0v} + 2\alpha^{(1)}_{im}T_{mn}\alpha^{(2)}_{nj}\mu^{(1)}_{0k}a^{(2)}_{rw}T_{wv}\mu^{(1)}_{0v}$$

$$+ 2\alpha^{(1)}_{im}T_{mn}\alpha^{(2)}_{nj}\mu^{(2)}_{0k}a^{(1)}_{rw}T_{wv}\mu^{(2)}_{0v} + 2\alpha^{(1)}_{ij}\mu^{(1)}_{0k}a^{(1)}_{rm}T_{mn}a^{(2)}_{nw}T_{wv}\mu^{(1)}_{0v}$$

$$+ 2\alpha^{(1)}_{ij}\mu^{(2)}_{0k}a^{(2)}_{rm}T_{mn}a^{(1)}_{nw}T_{wv}\mu^{(2)}_{0v} + 2\alpha^{(1)}_{ij}\mu^{(1)}_{0k}a^{(2)}_{rm}T_{mn}a^{(1)}_{nw}T_{wv}\mu^{(2)}_{0v}$$

$$+ 2\alpha^{(1)}_{ij}\mu^{(2)}_{0k}a^{(1)}_{rm}T_{mn}a^{(2)}_{nw}T_{wv}\mu^{(1)}_{0v} + \alpha^{(1)}_{im}T_{mn}\alpha^{(2)}_{nw}T_{wv}\alpha^{(1)}_{vj}\mu^{(1)}_{0k}\mu^{(1)}_{0r}$$

$$+ \alpha^{(1)}_{im}T_{mn}\alpha^{(2)}_{nw}T_{wv}\alpha^{(1)}_{vj}\mu^{(2)}_{0k}\mu^{(2)}_{0r} + 2\alpha^{(1)}_{im}T_{mn}\alpha^{(2)}_{nw}T_{wv}\alpha^{(1)}_{vj}\mu^{(1)}_{0k}\mu^{(2)}_{0r}\Big\}$$

$$\times\left\langle l^x_i l^x_j l^x_k l^x_r - l^y_i l^y_j l^y_k l^y_r\right\rangle, \tag{2.70}$$

and

$$\mu_1\beta_1 = \frac{2}{k_BT}\left\{\beta^{(1)}_{ijk}\mu^{(2)}_{0r}\right\}\left\langle l^x_i l^x_j l^x_k l^x_r - l^y_i l^y_j l^y_k l^y_r\right\rangle . \tag{2.71}$$

The final expressions of equations (2.61) to (2.69) are obtained by evaluating the isotropic averages using the standard results given in equation (2.15). The calculation of B_K requires the intermolecular potential energy so that numerical integration can be undertaken. Use can be made of the classical potential

$$U_{12}(\tau) = U_{LJ} + U_{\mu,\mu} + U_{\mu,\theta} + U_{\theta,\theta} + U_{\mu,ind\,\mu} + U_{\theta,ind\,\mu} + U_{shape} \tag{2.72}$$

where U_{LJ} is the Lennard-Jones 6:12 potential, $U_{\mu,\mu}$, $U_{\mu,\theta}$ and $U_{\theta,\theta}$ are the dipole-dipole, dipole-quadrupole and quadrupole-quadrupole interaction energies of the two molecules, and $U_{\mu,ind\,\mu}$ and $U_{\theta,ind\,\mu}$ are the dipole-induced-dipole and quadrupole-induced-dipole interaction energies of the two molecules. U_{shape} accounts for the angular dependence of the short-range repulsive force for non-spherical molecules.

$U_{\mu,\mu}$, $U_{\mu,\theta}$, $U_{\theta,\theta}$, $U_{\mu,ind\,\mu}$ and $U_{\theta,ind\,\mu}$ are symmetry dependent and can be expressed in terms of direction cosines via the Euler angles [3, 4]. The shape potential is given by

$$U_{shape} = 4\varepsilon\left(\frac{R_0}{R}\right)^{12}\left\{D_1[3\cos^2\beta_1 + 3\cos^2\beta_2 - 2] + D_2[3\sin^2\beta_1\cos^2\gamma_1 + 3\sin^2\beta_2\cos^2\gamma_2 - 2]\right\} \tag{2.73}$$

where the shape parameters D_1 and D_2 are dimensionless [3].

2.4 Interacting helium atoms

Semi-empirical calculations of B_K for the noble gases Ar, Kr and Xe have been performed by Hohm [10]. Precise *ab initio* quantum mechanical computations of B_K have

been performed for He [11, 12], and at our experimental temperatures and gas densities, the contribution of the B_K term to ${}_mK$ is of the order of 0.06%, which is well below the threshold of detectability by our apparatus. Consequently, any attempts at measuring density-dependent deviations from the ideal gas behaviour for helium would be futile.

REFERENCES

[1] J. Kerr, A new relation between electricity and light: Dielectrified media birefringent, *Phil. Mag.*, **50**, 337-348 (1875).

[2] A. D. Buckingham and J. A. Pople, Theoretical studies of the Kerr effect 1. Deviations from a linear polarization law, *Proc. Phys. Soc. A*, **68**, 905-909 (1955).

[3] V. W. Couling and C. Graham, Second Kerr effect virial coefficients of polar molecules with linear and lower symmetry, *Mol. Phys* **93**, 31-47 (1998).

[4] V. W. Couling, PhD thesis, Second light-scattering and Kerr-effect virial coefficients of molecules with linear and lower symmetry, University of Natal (1995).

[5] A. D. Buckingham, Theoretical studies of the Kerr effect 2. The influence of pressure, *Proc. Phys. Soc. A*, **68**, 910-919 (1955).

[6] L. D. Barron, Molecular light scattering and optical activity, Cambridge University Press, Cambridge (1982).

[7] G. Otterbein, *Phys. Z*, **35**, 249-265 (1934).

[8] A. D. Buckingham and B. J. Orr, Kerr effect in methane and its four fluorinated derivatives, *Trans. Faraday Soc.* **65**, 673-681 (1969)

[9] A. D. Buckingham, P. A. Galwas and L. Fan-Chen, Polarizabilities of interacting polar molecules, *J. Mol. Struct.*, **100**, 3-12 (1983).

[10] U. Hohm and L. Zarkova, Semi-empirical calculation of second Kerr-effect virial coefficients of atoms and small molecules, *Chem. Phys. Lett.*, **289**, 293-297 (2004).

[11] H. Koch, C. Hattig, H. Larsen, J. Olsen, P. Jorgensen, B. Fernandez and A. Rizzo, The effect of intermolecular interactions on the electric properties of helium and argon.

II. The dielectric, refractivity, Kerr, and hyperpolarizability second virial coefficients, *J. Chem. Phys.*, **111**, 10108-10118 (1999).

[12] W. Skomorowski and R. Moszynski, Kerr and Cotton-Mouton effects in atomic gases: a quantum-statistical study, *Mol. Phys.*, 1414-1429 (2013).

Chapter 3

Jones Calculus Analysis of the Experiment

3.1 Introduction

In the laboratory frame $O(x, y, z)$, the $z-$axis is along the direction of propagation of the light beam, which travels along the axis of the Kerr cell containing the birefringent medium. The $x-$axis is in the direction of the applied uniform electric field, with y perpendicular to it, and the azimuth of the linearly-polarized light beam emerging from the polarizer is at exactly $\frac{\pi}{4}$ radians relative to the $x-$axis: it is this azimuth which is taken as the reference relative to which the azimuths of the other optical elements are measured. The applied electric field inside the Kerr cell leads to the orthogonal electric vector components $\mathscr{E}_x$ and $\mathscr{E}_y$ of the propagating light wave experiencing refractive indices n_x and n_y respectively. The two components will emerge from the birefringent sample (of path length l) with a relative phase difference ϕ of

$$\phi = \frac{2\pi l}{\lambda}(n_x - n_y) \tag{3.1}$$

where λ is the wavelength of the light. The Kerr cell can be modelled as a linear retarder with a retardance of ϕ and an azimuth of 0 radians. The beam emerging from the Kerr cell is elliptically polarized, and is passed through a quarter-wave plate having its fast axis set to an azimuth of $\frac{\pi}{4}$. The beam will emerge linearly polarized but with an azimuth of $\frac{\pi}{4} + \frac{\phi}{2}$. The combined effect of the Kerr cell and the quarter-wave plate is a rotation

in the plane of polarization of the incident beam by $\frac{\phi}{2}$. ϕ is a very small angle, typical of the order of microradians, which means that it is not feasible to measure it by extinction at the analyzer. Instead, ϕ is modulated so that phase-sensitive detection techniques can be employed. A modulated optical rotator is required to cancel the $\frac{\phi}{2}$ rotation emerging from the quarter-wave plate. A Faraday cell has been used as the nulling cell, and is modelled as an optical rotator capable of rotating the plane of polarization of the light beam through a variable but precisely-known angle θ.

With the analyzer crossing the polarizing prism, the light intensity arriving at the photodiode detector due to the induced birefringence will be so small that the arising signal will be swamped by the background noise. The optical signal needs to be amplified by several orders of magnitude, which is best achieved by offsetting the azimuth of the analyzer prism by a small angle.

A full Jones calculus analysis of the electric-field-gradient-induced birefringence (EFGIB) experiment has been performed by Graham *et al.* [1]. This was achieved with the aid of a BASIC program specifically written to perform the required symbolic manipulations. The modulated light wave emerging from the birefringent sample in the presence of the applied electric field gradient oscillates at the same frequency as that of the voltage applied to the wire electrodes, whereas for the Kerr effect, which is a quadratic electro-optic effect, the light wave emerging from the birefringent sample in the presence of the applied electric field oscillates at twice the frequency of the applied voltage. A full Jones calculus analysis of the Kerr-effect experiment is now presented, using the formalism previously developed by Graham *et al.* [1, 2], and making use of the matrix manipulation facilities of the NCAlgebra package designed as an add-on to the commercial Mathematica symbolic manipulation program of Wolfram Inc.

3.2 Jones Calculus Analysis

Linear combinations of the unit and Pauli matrices can be used to construct the Jones matrices for particular optical components [3]. The Pauli matrices

$$\mathbf{I} = \begin{bmatrix} 1 & 0 \\ 0 & 1 \end{bmatrix}, \ \mathbf{i} = \begin{bmatrix} i & 0 \\ 0 & -i \end{bmatrix}, \ \mathbf{j} = \begin{bmatrix} 0 & 1 \\ 1 & 0 \end{bmatrix}, \ \mathbf{k} = \begin{bmatrix} 0 & i \\ i & 0 \end{bmatrix} \tag{3.2}$$

combine as follows:

$$\mathbf{i^2} = \mathbf{j^2} = \mathbf{k^2} = -\mathbf{I},$$

$$\mathbf{ki} = \mathbf{j}, \ \mathbf{jk} = \mathbf{i}, \ \mathbf{ij} = \mathbf{k}.$$

$$\mathbf{ik} = -\mathbf{j}, \ \mathbf{kj} = -\mathbf{i}, \ \mathbf{ji} = -\mathbf{k}. \tag{3.3}$$

A linear retarder of retardance ρ and azimuth φ has the Jones matrix [3]

$$\mathbf{J}(\rho, \varphi) = \cos\frac{\rho}{2}\,\mathbf{I} \ + \sin\frac{\rho}{2}\cos 2\varphi\,\mathbf{i} \ + \sin\frac{\rho}{2}\sin 2\varphi\,\mathbf{k}, \tag{3.4}$$

while an optical rotator having rotation ψ has the Jones matrix

$$\mathbf{R}(\psi) = \cos\psi\,\mathbf{I} \ + \ \sin\psi\,\mathbf{j}. \tag{3.5}$$

A polarizer having an azimuth of σ is given by

$$\mathbf{P}(\sigma) = \begin{bmatrix} \cos^2\sigma & \cos\sigma\sin\sigma \\ \cos\sigma\sin\sigma & \sin^2\sigma \end{bmatrix}. \tag{3.6}$$

A linearly-polarized light beam having azimuth η possesses a normalized Jones vector of

$$\nu_\eta = \begin{bmatrix} \cos\eta \\ \sin\eta \end{bmatrix}. \tag{3.7}$$

If the light entering the Kerr cell has a polarization azimuth of $\frac{\pi}{4}$, and the analyzer prism is offset from the crossed position by a small angle α, then the light leaving the analyzer will have a Jones vector of

$$\nu = \mathbf{P}\left(\tfrac{\pi}{4} + \alpha\right)\mathbf{M_n}\mathbf{M_{n-1}}\cdots\mathbf{M_1}\nu_\mathbf{0}, \tag{3.8}$$

where $\mathbf{M_1}$, $\mathbf{M_2}$, $\cdots$, $\mathbf{M_n}$ represent the Jones matrices for the rotator and the retarders in the optical cascade. The product of $\mathbf{M_n}\mathbf{M_{n-1}}\cdots\mathbf{M_1}$ can be expressed as a linear combination of the $\mathbf{I}, \mathbf{i}, \mathbf{j}$ and $\mathbf{k}$ matrices since they form a closed group under matrix multiplication:

$$\mathbf{M}_n\mathbf{M}_{n-1}\cdots\mathbf{M}_1 = a\mathbf{I} + b\mathbf{i} + c\mathbf{j} + d\mathbf{k}. \tag{3.9}$$

If the intensity of the light after passing through the polarizer is I_0, then the intensity of the light passing through the analyzer and reaching the photodiode detector is

$$I = \nu^*\nu I_0. \tag{3.10}$$

Making use of this result together with equations (3.6)-(3.9) yields

$$\frac{I}{I_0} = b^2 + c^2 + 2\alpha(ac + bd) + \alpha^2(a^2 - b^2 - c^2 + d^2), \tag{3.11}$$

where terms up to order α^2 have been retained. All that remains is to find the coefficients a, b, c and d for the optical train.

The entrance and exit Pockels-glass windows of the Kerr cell can each introduce a small strain-induced birefringence, and these are considered separately. Let the entrance window be treated as a linear retarder possessing a small retardance β_1 and an arbitrary

azimuth θ_1:

$$\mathbf{S}_1(\beta_1, \theta_1) = \cos\frac{\beta_1}{2}\mathbf{I} + \sin\frac{\beta_1}{2}\cos 2\theta_1\mathbf{i} + \sin\frac{\beta_1}{2}\sin 2\theta_1\mathbf{k}. \tag{3.12}$$

The exit window will have a similar expression:

$$\mathbf{S}_2(\beta_2, \theta_2) = \cos\frac{\beta_2}{2}\mathbf{I} + \sin\frac{\beta_2}{2}\cos 2\theta_2\mathbf{i} + \sin\frac{\beta_2}{2}\sin 2\theta_2\mathbf{k}. \tag{3.13}$$

The Kerr cell should behave as a linear retarder of retardance ϕ and azimuth 0. The electrodes in the Kerr cell should lie perfectly horizontal, i.e. along the $y-$axis, but have to be manually rotated to achieve this, so that allowance must be made for a small residual error γ in the azimuth of the applied electric field from 0 radians. The Jones matrix for the Kerr cell is then

$$\mathbf{J}_K(\phi, \gamma) = \cos\frac{\phi}{2}\mathbf{I} + \sin\frac{\phi}{2}\cos 2\gamma\mathbf{i} + \sin\frac{\phi}{2}\sin 2\gamma\mathbf{k}. \tag{3.14}$$

An ideal quarter-wave plate has a retardance of exactly $\frac{\pi}{2}$ radians for the required wavelength. In practice, the retardance may deviate by a few degrees from this ideal value. To account for this, the retardance is modelled as $\frac{\pi}{2} + \xi$ radians, where ξ can take either sign and can be larger than a degree. The quarter-wave plate converts the elliptically polarized light emerging from the Kerr cell back to a state of linear polarization, and this is achieved whether the fast axis is at an azimuth of $+\frac{\pi}{4}$ or $-\frac{\pi}{4}$ radians. A small offset ε from these positions must also be allowed for, yielding a Jones matrix of

$$\begin{aligned}\mathbf{J}_{\frac{\lambda}{4}}\left(\frac{\pi}{2} + \xi, \pm\frac{\pi}{4} + \varepsilon\right) = {} & \frac{1}{\sqrt{2}}\cos\frac{\xi}{2}\,\mathbf{I} - \frac{1}{\sqrt{2}}\sin\frac{\xi}{2}\,\mathbf{I} \mp \frac{1}{\sqrt{2}}\cos\frac{\xi}{2}\sin 2\varepsilon\,\mathbf{i} \\ & \mp \frac{1}{\sqrt{2}}\sin\frac{\xi}{2}\sin 2\varepsilon\,\mathbf{i} \pm \frac{1}{\sqrt{2}}\cos\frac{\xi}{2}\cos 2\varepsilon\,\mathbf{k} \\ & \pm \frac{1}{\sqrt{2}}\sin\frac{\xi}{2}\cos 2\varepsilon\,\mathbf{k}.\end{aligned} \tag{3.15}$$

The Jones matrix for the Faraday cell is

$$\mathbf{R}(\theta) = \cos\theta\ \mathbf{I} + \sin\theta\ \mathbf{j}. \tag{3.16}$$

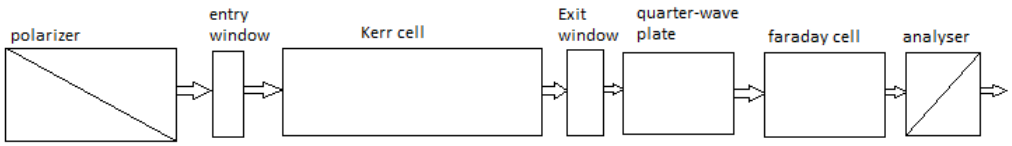

Figure 3.1: The components in the optical cascade which appear in the Jones calculus analysis.

The optical components in the cascade represented in Figure 3.1 are now used in the solution of equation (3.9), which becomes

$$\mathbf{R}(\theta)\ \mathbf{J}_{\frac{\lambda}{4}}\left(\frac{\pi}{2}+\xi, \pm\frac{\pi}{4}+\varepsilon\right)\ \mathbf{S}_2(\beta_2,\theta_2)\ \mathbf{J}_k(\phi,\gamma)\ \mathbf{S}_1(\beta_1,\theta_1) = a\mathbf{I} + b\mathbf{i} + c\mathbf{j} + d\mathbf{k}. \tag{3.17}$$

Multiplying out the matrices on the left-hand side of this equation yields 324 terms, many of which are small enough that their contribution is negligibe, and hence they can be safely discarded. The small angles in the remaining terms typically have the following magnitudes: ϕ, and hence θ, are of the order 10^{-6} radians, deliberate offsets in the analyzer or quarter-wave plate are less than $\frac{1}{2}^\circ$ so that ε and α never exceed 10^{-2} radians, the error in aligning the electrodes is less than 1° so that γ never exceeds 10^{-2} radians, while β_1 and β_2 are small enough that a safe upper limit of 10^{-2} radians can be ascribed to them.

In equation (3.11) for I/I_0, only those terms linear in the modulated quantities ϕ and θ are to be retained, since the phase-sensitive detector (PSD) filters out the higher harmonics. The coefficients of ϕ and θ will be terms in ε, α, γ, β_1 and β_2, and because none of

these angles exceeds 10^{-2} radians, the small angle approximations of $\cos x \approx 1 - \frac{1}{2}x^2$ and $\sin x \approx x$ can be made, where $x \in \{\varepsilon, \alpha, \gamma, \beta_1, \beta_2\}$. Equations (3.12) to (3.16) simplify to:

$$\mathbf{S}_1(\beta_1, \theta_1) = \mathbf{I} + C_1\mathbf{i} + S_1\mathbf{k}, \tag{3.18}$$

$$\mathbf{S}_2(\beta_2, \theta_2) = \mathbf{I} + C_2\mathbf{i} + S_2\mathbf{k}, \tag{3.19}$$

$$\mathbf{J}_K(\phi, \gamma) = \mathbf{I} + \frac{\phi}{2}\mathbf{i} + \phi\gamma\mathbf{k}, \tag{3.20}$$

$$\begin{aligned}\mathbf{J}_{\frac{\lambda}{4}}\left(\frac{\pi}{2} + \xi, \pm\frac{\pi}{4} + \varepsilon\right) = \frac{1}{\sqrt{2}}\cos\frac{\xi}{2}\,\mathbf{I} - \frac{1}{\sqrt{2}}\sin\frac{\xi}{2}\,\mathbf{I} \mp \sqrt{2}\varepsilon\cos\frac{\xi}{2}\,\mathbf{i} \\ \mp \sqrt{2}\varepsilon\sin\frac{\xi}{2}\,\mathbf{i} \pm \frac{1}{\sqrt{2}}\cos\frac{\xi}{2}\,\mathbf{k} \\ \pm \frac{1}{\sqrt{2}}\sin\frac{\xi}{2}\,\mathbf{k},\end{aligned} \tag{3.21}$$

and

$$\mathbf{R}(\theta) = \mathbf{I} + \theta\mathbf{j} \tag{3.22}$$

where

$$C_n = \frac{\beta_n}{2}\cos 2\theta_n, \qquad S_n = \frac{\beta_n}{2}\sin 2\theta_n. \tag{3.23}$$

Equation (3.11) yields

$$\frac{I}{I_0} = \phi\{C_1 + C_2 + \varepsilon(\mp\cos\xi + 2S_2 + 2S_2\sin\xi) + \alpha(\pm\cos\xi - 2S_2\sin\xi)\}$$

$$+\theta\ \{-2C_1S_1\sin\xi - 2C_2S_2\sin\xi - 4C_1S_2\sin\xi \pm 2C_1\cos\xi$$

$$\pm 2C_2\cos\xi + \varepsilon(-2 - 2\sin\xi) + 2\alpha\} \tag{3.24}$$

where the upper and lower signs correspond to the two possible quarter-wave plate azimuths ($+\frac{\pi}{4}$ and $-\frac{\pi}{4}$) respectively.

The value of θ which is equal to $\frac{\phi}{2}$ is called θ_{null}, being the rotation needed to null the induced birefringence in the Kerr cell in the case of ideal components in perfect orientations. As previously shown by Graham *et al.* [1] in the case of EFGIB, θ_{null} can be found from the intersection of two graphs of $\frac{I}{I_0}$ versus θ corresponding to two different offsets of the quarter-wave plate, these offsets preferably having similar magnitudes (of around 10^{-2} radians) and opposite signs. The value of θ for this intersection for the Kerr-effect experiment is the same as for the EFGIB experiment, and will be

$$\theta_{int} = \tfrac{1}{2}\phi\ \frac{\pm\cos\xi - 2S_2 - 2S_2\sin\xi}{1 + \sin\xi}, \tag{3.25}$$

which for small ξ is

$$\theta_{int} = \tfrac{1}{2}\phi\ \frac{\pm 1 - 2S_2}{1 + \xi}. \tag{3.26}$$

If the deviation ξ of the quarter-wave plate from an ideal retardance of $\frac{\pi}{4}$ is precisely known, then θ_{int} can be measured precisely provided S_2 is negligibly small. Unfortunately, the combined contributions of ξ and S_2 can account for as much as 10% to θ_{null} [1].

The preferable experimental technique is to fix the quarter-wave plate azimuth at either of the $\pm\frac{\pi}{4}$ settings. Then offsetting the analyzer prism to positions α_1 and α_2 (of

similar magnitude though opposite in sign) and plotting the two lines of $\frac{I}{I_0}$ versus θ will yield an intersection at

$$\theta_{int} = -\tfrac{1}{2}\phi(\pm\cos\xi - 2S_2\sin\xi). \tag{3.27}$$

Here, provided ξ is relatively small, the $2S_2\sin\xi$ term is at least two orders of magnitude smaller than the corresponding strain contribution $2S_2$ in equation (3.26), and can thus be safely ignored. A quarter-wave plate in which the retardance is very close to $\frac{\pi}{2}$ radians (to better than 1%) was used in this experimental project, so that $\cos\xi \approx 1$, equation (3.27) reducing to

$$\theta_{int} = \mp\tfrac{1}{2}\phi. \tag{3.28}$$

REFERENCES

[1] C. Graham, D. A. Imrie and R. E. Raab, Measurement of the electric quadrupole moments of CO_2, CO, N_2, Cl_2 and BF_3, *Mol. Phys.* **93**, 49-56, (1998).

[2] D. A. Imrie, PhD thesis, The measurement of electric quadrupole moments of gas molecules by induced birefringence, University of Natal (1993).

[3] R. Piazza, V. Degiorgio and T. Bellini, Matrix analysis of electric birefringence measurements, *Opt. Comm.* **58**, 400-404 (1986).

Chapter 4

Experimental Measurement of the Molar Kerr Constant

4.1 The measurement technique

The phase difference (or optical retardation) ϕ which arises from the birefringence which is induced in the fluid is the observable property which is measured in this Kerr effect experiment. The laboratory frame $O(x, y, z)$ is fixed relative to the Kerr electrodes, with the laser beam propagating along the $z-$direction, travelling between two parallel-plate electrodes across which are applied a uniform electric field. x is in the direction of this applied field, while y is perpendicular to it. A helium-neon laser supplies the monochromatic linearly-polarized light beam, the azimuth of which is precisely set by a calcite polarizing prism to be $\frac{\pi}{4}$ to the $x-$axis. When the Kerr cell is filled with a gas and an electric field is applied, the medium becomes birefringent. The component of the beam oscillating in the xz plane experiences a refractive index of n_x, which differs from the refractive index n_y as experienced by the component of the beam oscillating in the yz plane. Before the light beam enters the Kerr cell the components of the light vibrating parallel and perpendicular to the field are in phase with each other. After travelling through a birefringent gas sample having path length l, the beam emerges with an induced phase difference ϕ given by

$$\phi = \frac{2\pi l}{\lambda}(n_x - n_y), \tag{4.1}$$

where λ is the wavelength of the light.

The light emerging from the birefringent medium is elliptically polarized. The beam then passes through a quarter-wave plate having its fast axis set at $\frac{\pi}{4}$ to the $x-$axis, thereby converting the beam back to linearly-polarized light which has been rotated from the $\frac{\pi}{4}$ azimuth of the incident beam by $\frac{\phi}{2}$ radians. This linearly-polarized light is then passed through a Faraday cell, which rotates the plane of polarization of the beam back to $\frac{\pi}{4}$ relative to the applied electric field.

The magnitude of the induced phase difference is best determined by the technique of phase-sensitive detection since the phase difference is extremely tiny, typically around a millionth of a radian. This technique requires modulation of ϕ. The analyzer is initially crossed with the polarizer (before the electric field is applied to the gas sample). Upon application of the electric field, the signal arriving at the detector is brought to a minimum (or null) value by the compensating device consisting of the quarter-wave plate and Faraday cell. Attempting to achieve a null signal in this manner is exceptionally problematic, the light intensity reaching the photodiode detector being far too small to yield a signal that is distinguishable from the background noise. This problem is best overcome by offsetting either the analyzer or the quarter-wave plate by a small angle ε, thus introducing a small static retardation into the optical path, which produces an amplification of several orders of magnitude in the optical signal. This linear method of optical detection was introduced by Badoz in 1956 [1]. In our experiment, under the guidance of the Jones calculus analysis described in Chapter 3, the analyzer was the element which was offset.

The phase-sensitive detector (PSD) output is best measured and plotted as a function of the rms current which passes through the coils of the Faraday cell's solenoid. As first shown by Graham *et al.* in the case of electric-field-gradient-induced birefringence (EFGIB) [2], the null current is not necessarily the value corresponding to zero PSD output. The reason for this is that any strain birefringence which is present in the Pockels glass windows at the entrance and exit of the Kerr cell can cause an offset. A compre-

hensive Jones-calculus analysis of the elements in the optical train, and their effect on the polarization properties of the beam as it passes through each element, was performed by Graham *et al.* in the context of EFGIB [2]. This type of Jones-calculus analysis has been performed for the Kerr-effect (quadratic electro-optic) birefringence as part of this project. What is observed is that the straight lines obtained from plots of the PSD output versus the Faraday cell rms current, and optical rotation, for analyzer offsets of $+\varepsilon_1$ and $-\varepsilon_2$ intersect at a point the corresponding current of which is the null current. Again, as initially shown by Graham *et al.* for EFGIB, and as shown for the Kerr effect in this project, if the static retardation is introduced into the optical train by offsetting the quarter-wave plate, then any deviation, even small, from the ideal retardance for the wavelength of the transmitted light will lead to sometimes significant errors in the measured null currents, and hence in the extracted molar Kerr constants. It is for this reason that the analyzer is offset, rather than the quarter-wave plate.

The data-acquisition unit (DAU), which is controlled by a personal computer (PC), is used to monitor the PSD output. The recorded data is analyzed by the PC using an HP BASIC program which was originally written by Dr Couling and Mr Ntombela for their EFGIB experiment, and which was modified during the course of this project for the Kerr-effect experiment. The other electronic devices include the high-voltage power supply (which is used to supply the voltage to the electrodes by means of which the electric field is generated between them), as well as a frequency doubler and phase shifter (which ensure that the signal to the Faraday cell is of the same frequency as that from the Kerr cell, and exactly in anti-phase to it). All electronic and optical components associated with the experiment are shown in the block diagram overleaf.

In this experiment the measurement of the induced phase difference, and calculation of the molar Kerr constant, from the collected data is performed by the HP BASIC computer program. Not every aspect of the experiment is automated and under computer control. Some of the tasks which are performed manually include the calibration of the high voltage power supply and the pressure transducer. Another parameter which needs to be adjusted manually is the phase of the rms current flowing through the coils of the

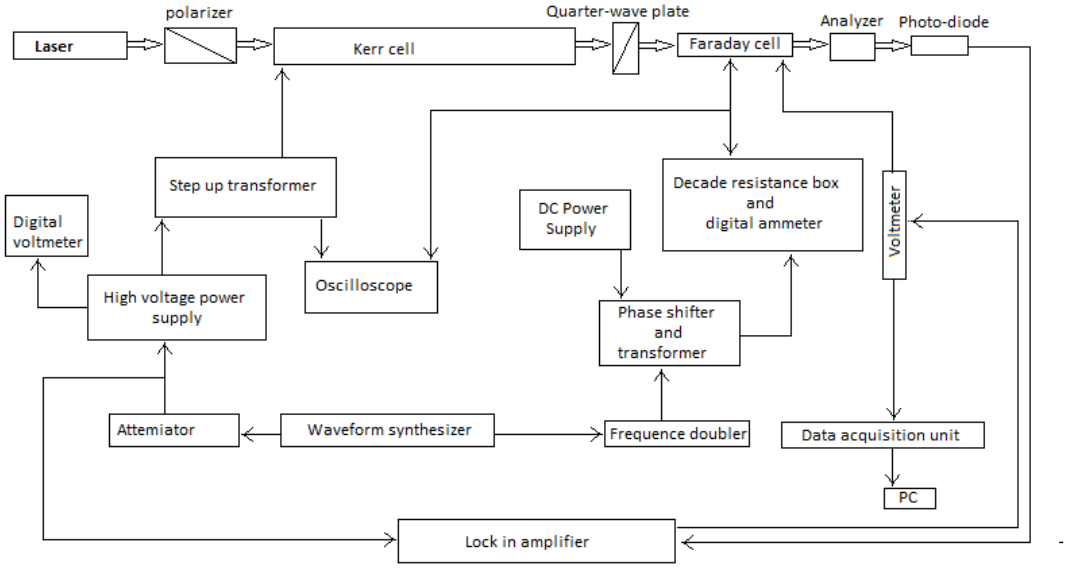

Figure 4.1: The block diagram of the experimental setup.

Faraday cell relative to that of the voltage applied to the Kerr electrodes. This phase adjustment is performed before each experimental run to minimize drifts, and is attained through the aid of Lissajous figures displayed on an oscilloscope.

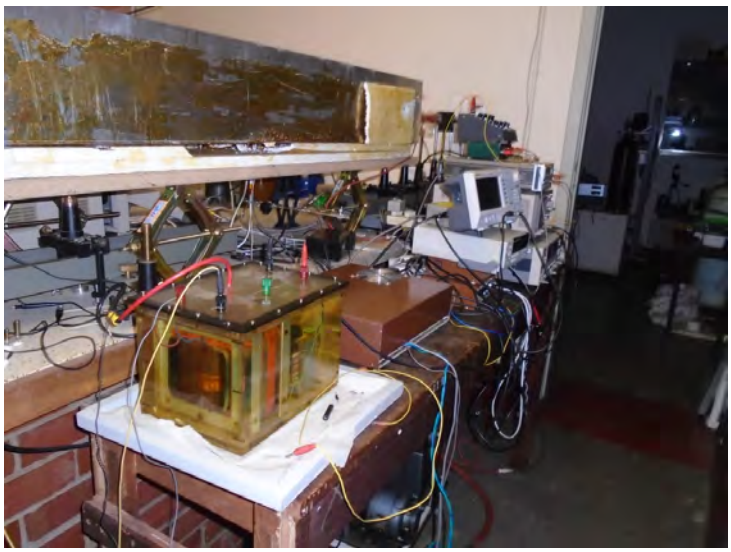

Figure 4.2: A photograph of the laboratory.

4.2 The supporting bench

In our experiment, where retardances of the order of microradians are measured, it is crucial that mechanical vibrations be kept to a minimum, since any mechanical vibration while the experiment is running will introduce excess contributions to the already-large signal noise. A cast iron optical bench is supported by a vibration-damped concrete slab of dimensions 4 m by 25 cm with a height of 60 cm. The concrete slab rests upon a vibration-damping cork foundation of 10 cm. Another concrete slab 123 cm in length, also resting on a cork foundation, is joined perpendicular to the main bench so that they form a T-shape. This increases the stability of the entire concrete slab. The cast-iron optical bench is 4 m long, 23 cm wide and 9 cm high, and is made from mild-steel C-bar with a stabilizing side arm, all resting on anti-vibration pads. The optical components, including the laser, polarizer, quarter-wave plate, Faraday cell, analyzer and photodiode detector, were attached to the optical bench by means of magnetic bases, while the Kerr cell was held by an adjustable brass screw-held system.

4.3 The Optical Components

4.3.1 The laser

A Melles-Griot 1145P linearly-polarized He-Ne laser was used throughout this experiment. A 35 mW continuous-wave monochromatic beam of wavelength 632.8 nm is produced. The laser was supported by magnetic bases which had fine-control adjustors, allowing for fine directional adjustment, thus providing for precise alignment of the beam.

Two irises were initially used to align the laser beam to travel parallel to the optical rail, after which the other optical components and the Kerr cell were put in place. Once the cell was placed inside the oven, to avoid the possibility of having multiple reflections from the electrode surfaces, the cell was carefully adjusted to make sure that the light beam travelled parallel to the electrodes, and in between them.

Figure 4.3: The laser.

4.3.2 The polarizer

A Glan-Thompson prism with an extinction ratio of 10^6 was used in this experiment. The polarizing prism was housed in a divided circle having a resolution of $2'$ of arc. The prism housing was attached to an aluminum rod, which was placed in a magnetic holder and locked onto the optical bench.

The light emerging from the laser is almost linearly polarized and the laser is rotated to allow the electric vector of the light wave to vibrate in a plane at $\frac{\pi}{4}$ radians to the vertical. The light is passed through the polarizer wich has its transmission axis set precisely at $\frac{\pi}{4}$ to the vertical. This arrangement ensures that the components of the light wave parallel and perpendicular to the applied electric field are equal in magnitude.

4.3.3 The quarter-wave plate

A zero-order quarter-wave plate (Newport 05RP04) with a retardance of $(\frac{\pi}{2} \pm 1\%)$ radians for a wavelength of 632.8 nm was used in this work. The quarter-wave plate is responsible for converting the elliptically-polarized light emerging from the Kerr cell back into linearly-polarized light. It is housed in a divided circle similar to that of the polarizer. The fast axis of the quarter-wave plate is set fixed at $\frac{\pi}{4}$ to the vertical.

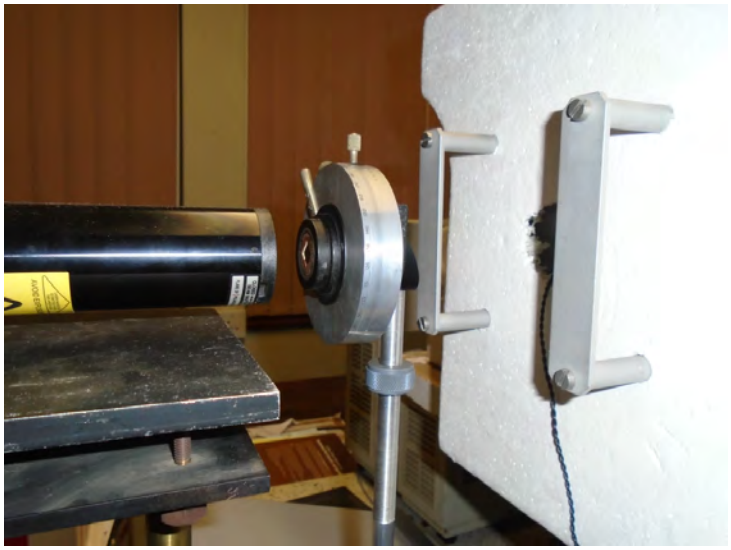

Figure 4.4: The polarizer.

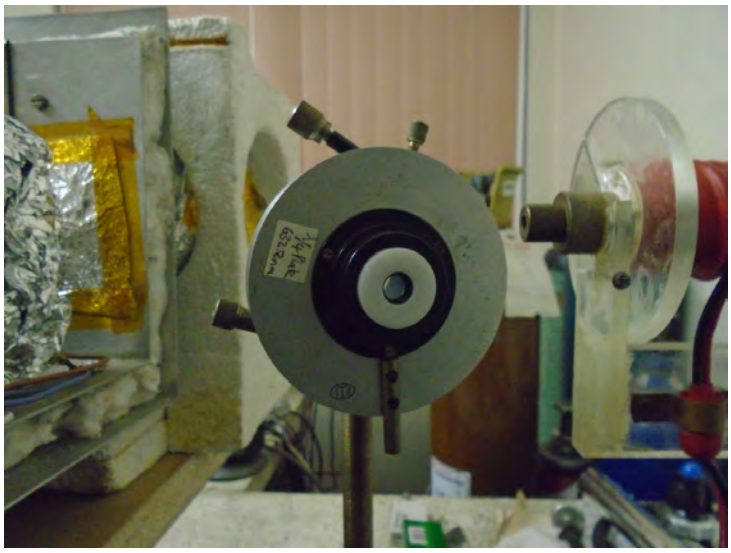

Figure 4.5: The quarter-wave plate.

4.3.4 The Faraday cell

The quarter-wave plate together with the Faraday cell are used to compensate the phase difference induced in the light beam after propagating through the birefringent gas sample contained in the Kerr cell. The linearly-polarized light emerging from the quarter-wave plate is offset from the $+\frac{\pi}{4}$ position by $\frac{\phi}{2}$ (i.e. by half the induced phase difference), and is rotated back to a null position using the Faraday cell. The amount of rms current

required by the Faraday cell coil to rotate the linearly-polarized light back to its null position can in principle be used to determined the induced phase difference, provided the Faraday cell has been accurately and precisely calibrated.

The Faraday cell consists of a solenoid coil of heavy-gauge copper wire surrounding a glass tube containing a sample of ultra-high-purity water.

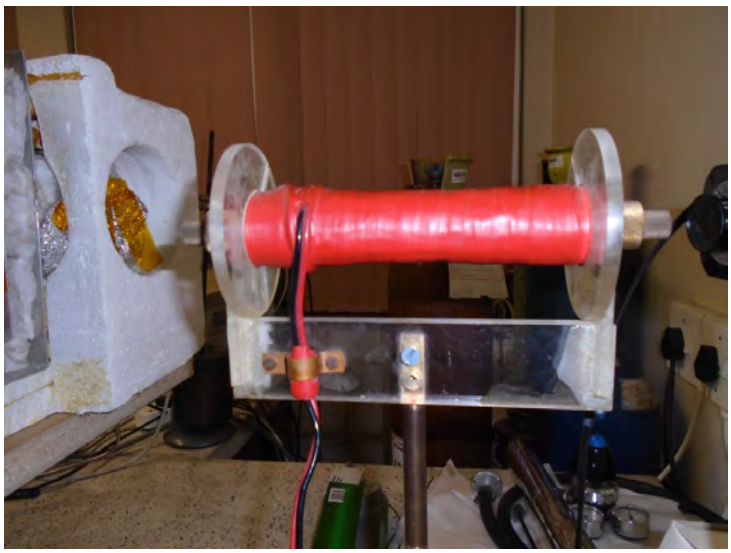

Figure 4.6: The Faraday cell.

4.3.5 The Analyzer

The light intensity reaching the detector needs to be brought to a minimum value, which was achieved by offsetting the analyzer. The analyzer is housed in a Newport CONEX-AG-PT100P precision rotation stage, comprising a piezo-driven device and closed-loop controller which has a very accurate bi-directional repeatability of 0.003°, uni-directional repeatability of 0.002° and a minimum incremental motion of 0.001°. The PC controls the precision rotator by sending commands to the Agilent 34907A data-acquitition unit (DAU), and offsets the analyzer by 0.5° rotations of $+\varepsilon_1$ and $-\varepsilon_2$ to achieve the introduction of a static retardation into the optical train. This allows for implementation of Badoz's linear method of optical detection.

Figure 4.7: The analyzer.

4.3.6 The Detector

The photodiode detector is the last element in the optical cascade, and is placed near the end of the optical bench. It is a silicon photodiode, UDT Sensors model FIL100V0248. The photodiode detector is connected to a Stanford Research Systems SR830 phase-sensitive detector by means of a screened coaxial cable, and is used to measure the intensity of the modulated light beam emerging from the analyzer.

Figure 4.8: The photodiode detector.

4.4 The Kerr cell

The Kerr cell contains the electrodes and the gas under investigation. A bulkhead allows for connection of the high voltage to the electrodes, and is designed to minimize the possibility of electrical breakdown. To allow for a range of gases to be investigated, the cell is designed to be as chemically inert as possible, and so is constructed from 316-stainless steel. A stainless-steel cylinder 1.500 m in length, 54.4 mm in internal diameter and with a wall thickness of 3.8 mm has been used. Flanges 10.5 cm in diameter are welded on both ends of the cell to allow end caps to be bolted in place. Two flat stainless steel discs were used as the end caps, each having a diameter 10.5 cm and a thickness of 1.0 cm, with a central hole of 0.5 cm. Two small disks having 0.5 cm central holes were used to hold the Pockels glass windows against the caps. Teflon washers served as seals between the glass and the steel surfaces.

The electric field was generated between the electrodes by applying an ac voltage to one of the electrodes while the other electrode was grounded together with the outer cell. The electrodes are parallel to each other, having a length of 1.468 m and width of 3.2 cm, with an average spacing of (3.108 ± 0.012) mm. Small blocks of Macor ceramic serve as electrode spacers. The electrodes were machined and polished to be flat and smooth, to ensure that the electric field is uniform throughout the pathlength of the electrodes.

All the components used in the experiment need to be absolutely clean, so the electrodes were washed with soap solution followed by a number of rinses with distilled water, then ethanol, followed by acetone and trichloroethylene. The electrodes were then positioned inside the cell, which in turn was placed into the oven.

4.5 The oven

Temeperature control of the Kerr cell is achieved by means of an oven, which can heat the cell to an upper temperature of around 250°C. This oven consists of a 1.5 kW heater element cut in two, the pair being connected in series along either side of the cell, placed inside an oven constructed from two layers of sheet metal with a 5 cm layer of insulating fibre-glass wool in between them. The heater elements are powered directly off the

mains supply, and temperature control is achieved through an Autonomics TZN4S PID controller. The oven could be maintained at a particular temperature to within a degree. Three platinum PT100 RTDs monitor the temperature inside the oven, and are evenly spaced along the length of the cell so that the average temperature inside the oven can be monitored.

4.6 Data acquisition and computer control system

The experiment was fully automated by means of the Agilent DAU, which was linked to the PC via an IEEE interface. An HP BASIC computer program was used to instruct the DAU to record the rms high voltage applied to the Kerr cell electrodes, the ac current passing through the Faraday cell, the average oven temperature as measured by three widely-spaced PT100s, the PSD output voltage and the pressure transducer output voltage. The program would also, when appropriate, instruct the DAU to set the rms current flowing through the Faraday cell solenoid coils, or rotate the rotation stage, and hence set the analyzer to its desired azimuth.

The light emerging from the analyzer impinges upon the photodiode detector, the output of which is monitored by an SRS830 PSD. The PSD output signal is measured by the DAU. The analyzer was successively rotated to its $+\varepsilon_1$ and $-\varepsilon_2$ settings using the piezo motor rotation stage (PMRS). The PMRS provides a continuous rotation, and can be set to a large number of precisely repeatable positions. The DAU adjusts the ac current flowing through the Faraday cell's solenoid coils by sending instructions to a remote gain control to provide ac output to a power amplifier connected across the coil. For each of the analyzer offsets, ten equally spaced PSD voltage readings were provided by adjusting the rms current through the Faraday cell. Full details of the HP BASIC program controlling the experiment are given in Appendix B.

4.7 Required Calibrations

4.7.1 Pressure transducer calibration

A Gems 2200 series 60 bar pressure transducer was used to measure the gas pressure in the cell. The pressure transducer was powered by a 10 V dc supply, and it was calibrated using a Budenberg dead-weight pressure tester. Oxygen gas was allowed into the system via the gas inlet valves, and the plot of the resulting dead-weight pressure vs transducer voltage is provided in Figure 4.9.

Table 4.1: Calibration data for the Gems pressure transducer.

Pressure transducer output voltage (V)	Pressure (kPa)
0.9982	103
1.2656	503
1.6659	1101
1.9990	1601
2.3318	2100
3.0642	3201
3.3280	3595
3.6595	4094
4.3226	5093

4.7.2 High-voltage calibration

The electric field in the cell is generated by applying a high voltage to one of the Kerr electrodes, keeping the other grounded. This high voltage is obtained from a 125 W power amplifier which drives a step-up tranformer with a turns ratio of 1000:1. This primary transformer's output is applied to the electrode using the teflon-insulated high tension throughput via the bulkhead connector. A secondary transformer is used to step down the signal by 1000 times before being fed back to the high-voltage power supply.

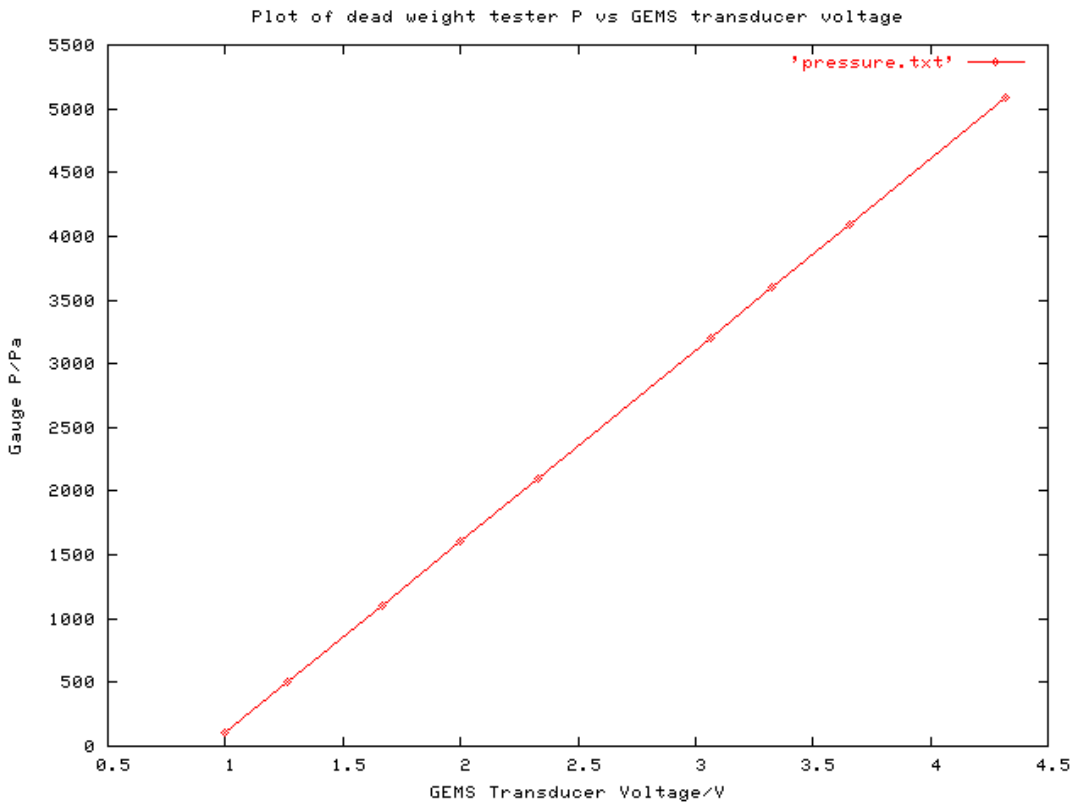

Figure 4.9: Plot of dead weight tester pressure versus Gems pressure-transducer voltage

This allows the power supply to continuously monitor its driving signal, a feedback loop serving to maintain the output at a constant level to within 0.1%. A precision rectifier converts part of the feedback signal into a dc signal so that 1 V dc output corresponds to 1000 V rms ac signal on the high-voltage output. This allows the ac voltage applied to the electrode to be monitored and recorded by the PC via the DAU.

The calibration of the high-voltage power supply was performed by means of varying the high-voltage power supply up to 1000 V rms while recording the corresponding voltage. A Hewlett-Packard 34401A $5\frac{1}{2}-$digit multimeter was used to measure the rms ac signal while a Fluke 45 Dual Display multimeter was used to record the corresponding dc voltage. The results are tabulated below, and the calibration graph is presented.

During an experimental run, the DAU records the dc voltage from the precision rectifier, and the HP BASIC program then calculates the rms ac voltage that is applied to the electrode of the Kerr cell using this calibration curve.

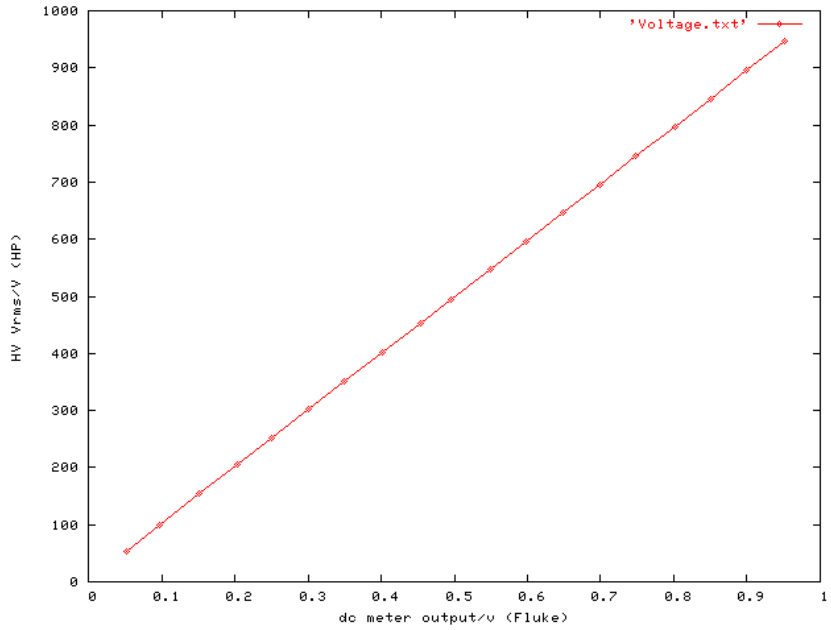

Figure 4.10: Plot of the rms high voltage versus the dc precision rectifier voltage.

4.7.3 Faraday cell calibration

Precise and accurate calibration of the Faraday cell is of great importance, since this calibration factor is used in the calculations to convert the measured null current into an optical rotation and thereby to determine the molar Kerr constant of a particular gas sample. The calibration of the Faraday cell was thus fully automated using an HP BASIC program provided in Appendix B2. This program would command the DAU to send instructions to the remote gain control to provide the required ac output to a power amplifier which is connected across the Faraday cell's solenoid coil. The ac current induces a rotation in the plane of the linearly-polarized beam propagating though the Faraday cell. The polarizer and the analyzer are then crossed by rotating the analyzer prism using a Newport CONEX-AG-PT100P precision rotator until the PSD output is zero. The Faraday calibration constant was determined from a least-squares fit of the analyzer rotation in radians versus the rms ac current. The calibration was repeated over several days, and an average result was obtained. The calibration data is tabulated below, and yields a calibration constant of $K_F = (0.62280 \pm 0.00068) \times 10^{-6}$ rad mA^{-1}.

Table 4.2: Calibration data for the high voltage transformer.

dc meter/V	HV Vrms/V
0.05190	53.96
0.09754	99.91
0.15164	153.61
0.20321	204.90
0.24984	251.09
0.30119	302.02
0.3504	350.73
0.4017	401.57
0.4535	452.81
0.4948	493.66
0.5489	547.55
0.5979	596.17
0.6492	646.97
0.6983	695.53
0.7480	744.90
0.8015	797.91
0.8504	846.39
0.8998	895.25
0.9513	946.33

Table 4.3: Calibration data for the water Faraday cell.

No of runs	Average calibration constant K_F/mA	Standard Deviation
53	0.6222	0.0064
55	0.6237	0.0059
54	0.6230	0.0064
46	0.6232	0.0064
45	0.6221	0.0070
mean	0.62280	0.00068

REFERENCES

[1] J. Badoz, Mesures photoelectriques de faibles birefringences et de tres petits pouvoirs rotatoires, *J. Phys. Radium*, **17**, A143-A149 (1956).

[2] C. Graham, D. A. Imrie and R. E. Raab, Measurement of the electric quadrupole moments of CO_2, CO, N_2, Cl_2 and BF_3, *Mol. Phys.* **93**, 49-56, (1998).

Chapter 5

Results and Discussion

5.1 Measurement of γ^K of helium

The second Kerr hyperpolarizability γ^K of helium at the wavelength 632.8 nm has been the subject of several independent experimental Kerr-effect investigations [1–3]. The measurements of ${}_mK$ for helium reported in this dissertation were obtained using ultra-high-purity He with a quoted minimum purity of 99.999%, supplied by Afrox. The second and third pressure virial coefficients required to calculate the molar volume of the gas samples were taken from the tabulations of Dymond *et al.* [4]. The refractive indices were calculated from Landolt-Börnstein tables [5] together with these molar volumes. The dielectric constant ε_r was calculated using the Clausius-Mosotti function expanded in terms of inverse molar volume,

$$\frac{\varepsilon_r - 1}{\varepsilon_r + 2} V_m = A_\varepsilon + \frac{B_\varepsilon}{V_m} + \frac{C_\varepsilon}{V_m^2} + \cdots , \tag{5.1}$$

where A_ε and B_ε are the first and second dielectric virial coefficients respectively, and V_m is the molar volume. Use was made of the dielectric virial coefficient data measured by Schmidt *et al.* [6].

5.2 Results

The Kerr cell was baked out for several days while under vacuum and heated at 150°C. This was done to facilitate the removal of any adsorbed molecules which could later con-

taminate the helium sample, these molecules making a much higher contribution to ${}_mK$ than helium, so that even small traces of such impurities could affect the measurements. 82 experimental runs were performed at 399.4 K, and 32 runs at 445.7 K. These measured data are presented in tables 5.1 and 5.2 respectively, and yield $\gamma^K = (2.944 \pm 0.076) \times 10^{-63}$ $C^4m^4J^{-3}$ and $\gamma^K = (2.946 \pm 0.097) \times 10^{-63}$ $C^4m^4J^{-3}$ respectively. The theoretical value for γ^K was calculated by Bishop *et al.* [7] using the CI-Hylleraas *ab initio* quantum mechanical procedure, this result being accurate to within 0.1%. At our experimental wavelength of 632.8 nm, they obtained $\gamma^K = (2.757 \pm 0.003) \times 10^{-63}$ $C^4m^4J^{-3}$. Our average measured value agrees to within 6.8%, and is compared with the measured Kerr-effect second hyperpolarizabilities of other researchers in Table 5.3.

Table 5.1. The Kerr effect null currents for helium measured at 399.4 K and 632.8 nm.

Null current (mA)	Temperature (°C)	High Voltage (kV)	Pressure (kPa)
-1.003	126.27	5.0689	4561.8
-0.976	126.25	5.0692	4560.8
-0.963	126.41	5.0695	4560.0
-0.975	126.28	5.0697	4559.8
-0.985	126.51	5.0698	4559.5
-0.921	126.42	5.0701	4557.9
-1.010	126.12	5.0702	4557.0
-0.945	126.41	5.0702	4556.4
-0.949	126.47	5.0703	4555.5
-1.016	126.30	5.0704	4555.3
-0.982	126.35	5.0703	4554.3
-0.943	126.32	5.0705	4553.2
-0.960	126.24	5.0706	4551.3
-0.974	126.25	5.0708	4550.7
-0.972	126.38	5.0709	4550.2
-0.953	126.14	5.0709	4550.6
-0.948	126.19	5.0710	4549.4
-0.999	126.36	5.0711	4547.3
-0.969	126.30	5.0714	4547.5
-1.028	126.56	5.0712	4547.8
-0.942	126.43	5.0713	4547.1
-0.968	126.22	5.0715	4546.3
-0.986	126.36	5.0715	4544.5
-0.961	126.11	5.0716	4543.3
-0.982	126.31	5.0715	4542.4
-0.966	126.45	5.0715	4541.5
-0.994	126.37	5.0715	4540.9
-0.966	126.23	5.0717	4540.4
-0.999	125.98	5.0717	4539.2
-0.970	126.20	5.0717	4537.3

-0.989	126.31	5.0716	4537.2
-0.956	126.28	5.0719	4536.2
-0.968	126.43	5.0718	4536.2
-0.950	126.11	5.0720	4535.1
-1.006	126.16	5.0721	4534.5
-0.954	126.20	5.0718	4534.4
-0.947	126.30	5.0719	4533.9
-0.947	126.12	5.0718	4533.0
-0.963	126.46	5.0721	4532.2
-1.000	126.23	5.0721	4530.1
-0.960	126.18	5.0720	4529.4
-0.999	126.32	5.0721	4529.6
-0.929	126.36	5.0721	4528.7
-0.908	126.34	5.0721	4528.3
-0.977	126.34	5.0720	4527.4
-0.981	126.14	5.0722	4526.5
-0.955	126.11	5.0721	4525.2
-0.959	126.27	5.0722	4524.1
-0.946	126.23	5.0723	4524.1
-0.977	126.10	5.0723	4522.9
-0.956	126.39	5.0724	4522.6
-0.964	126.29	5.0722	4520.8
-0.987	126.35	5.0723	4520.0
-0.971	126.21	5.0724	4520.0
-0.971	126.31	5.0723	4520.1
-0.965	126.21	5.0722	4519.9
-0.957	126.08	5.0724	4516.5
-0.980	126.32	5.0724	4516.3
-0.922	126.12	5.0725	4515.7
-0.966	126.06	5.0725	4514.8
-0.963	126.21	5.0725	4513.8
-1.001	126.14	5.0725	4513.3

	-0.996	126.23	5.0725	4512.4
	-0.942	126.38	5.0723	4512.2
	-0.954	126.16	5.0725	4511.8
	-0.957	126.17	5.0725	4511.0
	-0.969	126.13	5.0726	4509.3
	-0.982	126.24	5.0726	4508.3
	-0.985	126.36	5.0726	4508.8
	-0.985	126.26	5.0726	4508.3
	-0.954	126.24	5.0726	4507.6
	-0.995	126.14	5.0725	4507.1
	-0.969	126.05	5.0726	4505.9
	-0.969	126.13	5.0728	4504.6
	-0.953	126.14	5.0725	4504.1
	-0.988	126.11	5.0726	4503.5
	-0.967	126.24	5.0727	4502.0
	-0.989	126.04	5.0726	4501.6
	-0.993	126.23	5.0726	4500.2
	-0.983	126.34	5.0726	4499.4
	-0.941	126.39	5.0728	4499.6
	-0.959	126.27	5.0728	4497.9
mean	-0.970	126.26	5.0718	4529.9
std dev	-0.022	0.12	0.0010	18.7

Table 5.2. The Kerr effect null currents for helium measured at 445.7 K and 632.8 nm.

	Null current (mA)	Temperature (°C)	High Voltage (kV)	Pressure (kPa)
	-0.806	172.87	5.1032	4168.90
	-0.808	172.73	5.1036	4168.31
	-0.836	172.39	5.1037	4167.13
	-0.816	172.29	5.1036	4166.19
	-0.834	172.35	5.1043	4166.68
	-0.809	172.47	5.1041	4163.81
	-0.823	172.54	5.1042	4163.12
	-0.821	172.62	5.1036	4161.18
	-0.816	172.66	5.1042	4161.51
	-0.833	172.45	5.1039	4159.24
	-0.835	172.46	5.1047	4159.65
	-0.810	172.37	5.1044	4159.04
	-0.842	172.49	5.1048	4158.52
	-0.807	172.46	5.10433	4157.20
	-0.829	172.44	5.1049	4155.67
	-0.828	172.40	5.1044	4153.65
	-0.800	172.24	5.1048	4154.67
	-0.839	172.37	5.1046	4151.94
	-0.805	172.40	5.1047	4154.11
	-0.847	172.38	5.1040	4152.73
	-0.809	172.42	5.1044	4151.68
	-0.823	172.71	5.1050	4151.89
	-0.826	172.64	5.1046	4151.02
	-0.817	172.62	5.1048	4151.47
	-0.831	172.86	5.1046	4149.23
	-0.812	172.61	5.1046	4147.64
	-0.841	172.58	5.1052	4147.59
	-0.811	172.34	5.1048	4146.98
	-0.830	172.64	5.1052	4147.08
	-0.817	172.48	5.1041	4143.56
	-0.811	172.83	5.1051	4143.55
	-0.828	172.79	5.1049	4143.59
mean	-0.822	172.53	5.1045	4155.5
std dev	-0.013	0.17	0.0005	7.6

Table 5.3. A comparison of measured and computed γ^K values for He at 632.8 nm.

$10^{63}\gamma^K$ ($C^4m^4J^{-3}$)	Method	Reference
3.22 ± 0.50	Kerr effect measurement	[1]
3.34 ± 0.25	Kerr effect measurement	[2]
2.762 ± 0.050	Kerr effect measurement	[3]
2.945 ± 0.097	Kerr effect measurement	this work
2.757 ± 0.003	CI-Hylleraas calculation	[7]

5.3 Discussion

The measured mean $\gamma^K = (2.945 \pm 0.097) \times 10^{-63}$ $C^4m^4J^{-3}$ obtained in this project is 6.8% larger than the accurate CI-Hylleraas *ab initio* calculation of Bishop *et al.* This is to be contrasted with the excellent agreement achieved by Tammer *et al.* [3], whose experimentally-determined $\gamma^K = (2.762 \pm 0.050) \times 10^{-63}$ $C^4m^4J^{-3}$ agrees with the *ab initio* computed value to within 0.2%. Their excellent agreement between experiment and theory bears some explanation.

In 1990, Tammer and Hüttner presented Kerr effect measurements of molecular hydrogen [8], extracting a measured γ^K for H_2 which is 9% smaller than the *ab initio* computed value of Bishop *et al.* [9]. These researchers were perturbed by this discrepancy, and gave considerable thought to possible systematic errors in their experiment. They eventually decided to verify the field integral of their Kerr cell, which had been obtained using the traditional method of determining E from applied voltage and electrode plate separation. Their verification procedure was based upon measurements of the rotational Stark effect in the millimeter wave spectrum of the OCS molecule. The calibration resulted in a revised field integral, which when applied to their H_2 experimental data from [3], resulted in the excellent agreement between experiment and theory found in Table 5.3. The discrepancy between the two field integrals was accounted for by the cumulative effect of small deviations from perfect flatness of the electrode surfaces.

In this project, E has been obtained from knowledge of the applied voltage and the electrode plate separation. It is possible that this estimate of E is erroneous for reasons similar to those experienced by Tammer and Hüttner, and this will need to be verified

by undertaking a Stark effect study using our electrode array. Such a study is a research project in its own right, and is well beyond the scope of the present investigation.

5.4 Future Work

This MSc project is an important first step in assembling and characterizing a Kerr-effect apparatus that will provide new measurements of the molar Kerr constants of gaseous species which are of increased accuracy and precision. Future work will entail measurement of the field integral using Stark effect spectroscopy. This will enable re-analysis of the γ^K data presented here. If sufficient agreement between experiment and theory is then attained, a series of measurements of ${}_mK$ for He will enable the statistical uncertainty of the measured γ^K to be reduced to the 0.1% level, so that direct comparison with the *ab initio* calculated value can be made at a level of precision commensurate with that of the computed value.

Once the Kerr-effect apparatus has been definitively calibrated using He as a primary reference standard, the goal is to proceed with measurements on a range of gaseous species. This will allow for the determination of precise and accurate (hyper)polarizabilities, as well as second Kerr-effect virial coefficients. Precise B_K data will allow for a stringent comparision with the calculated values obtained from the molecular-tensor theory reviewed here. This should provide useful insights into these intermolecular interaction effects.

REFERENCES

[1] L. L. Boyle, A. D. Buckingham, R. L. Disch and D. A. Dunmur, Higher polarizability of the helium atom, *J. Chem. Phys.*, **45**, 1318-1323 (1966).

[2] A. D. Buckingham and D. A. Dunmur, Kerr effect in inert gases and sulphur hexafluoride, *Faraday Trans.*, **64**, 1776-1783 (1968).

[3] R. Tammer, K. Löblein, K. H. Petting and W. Hüttner, Field calibrated measurements of the dc Kerr constants of helium and molecular hydrogen, *Chem. Phys.*, **168**, 151-158 (1992).

[4] J. H. Dymond, K. N. Marsh, R. C. Wilhoit and K. C. Wong, The virial coefficients of pure gases and mixtures, Springer-Verlag, Berlin (2002).

[5] Landolt-Börnstein, Zahlenwerte und Funktionen, edited by K.-H. Hellwege and A. M. Hellwege, Springer-Verlag, Berlin (1962) Band II, Teil 8.

[6] J. W. Schmidt, R. M. Gavioso, E. F. May and M. R. Moldover, Polarizability of helium and gas metrology, *Phys. Rev. Lett.*, **98**, 254504 (2007).

[7] D. M. Bishop and J. Pipin, Improved dynamic hyperpolarizabilities and field-gradient polarizabilities for helium, *J. Chem. Phys.*, **91**, 3549-3560 (1989).

[8] R. Tammer and W. Hüttner, The anisotropy of the second hyperpolarizability of molecular hydrogen from the pressure and temperature dependence of the Kerr effect, *Chem. Phys.*, **146**, 155-163 (1990).

[9] D. M. Bishop, J. Pipin and S. M. Cybulski, Theoretical investigation of the nonlinear optical peopreties of H_2 and D_2 - extended basis set, *Phys. Rev. A*, **43**, 4845-4853 (1991).

Appendices

Appendix A

A.1 The Euler angles and the $T-$tensors.

The relative orientation of an interacting pair of molecules under the influence of a static applied electric field E_i is shown in figure A.1.1 below

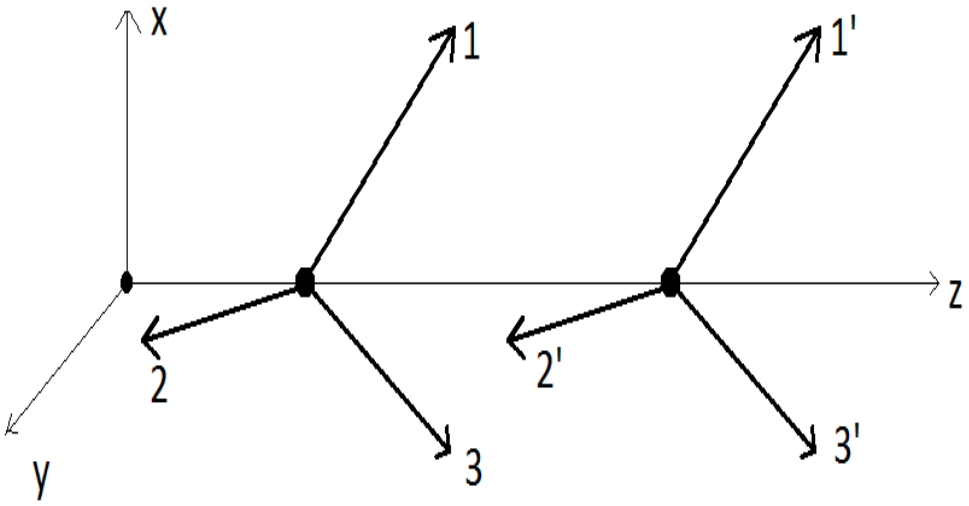

Figure A.1.1 Molecule-fixed axes $O(1,2,3)$ and $O(1',2',3')$ of the interacting pair of molecules 1 and 2 respectively. The space-fixed axes are $O(x,y,z)$.

The space-fixed axes are defined by the direction of the applied electric field E_x. The molar Kerr-constant determinations are performed in space-fixed axes, while if the symmetry of the molecule is to be exploited, its physical property tensors must be referred to a system of molecule-fixed axes. Since the molecules are tumbling around in space, their molecule-fixed axes are continually changing with respect to the space-fixed axes. The average projection of a molecule's tensor properties in the space-fixed axes is then obtained by referring the molecular-property tensors to molecule-fixed axes, and then projecting them into the space-fixed axes and averaging the projection over the orientational motion of the molecule.

As before, the Greek tensor subscripts are used to denote the tensor in the space-fixed axes while i, j, k and i', j', k' denote the tensors for molecules 1 and 2 expressed in their own system of molecule-fixed axes as illustrated in figure A.1.1. Nine direction cosines l_i^α are required to describe the relative orientation of each set of molecule-fixed axes and the space-fixed axes. Euler angles can be used to describe an arbitrary rotation of a system of Cartesian axes about its origin [1]. For molecule 1, the nine direction cosines l_i^α can be expressed as functions of three Euler angles α_1, β_1 and γ_1 as follows:

$$l_i^\alpha = \begin{bmatrix} \cos\gamma_1 & \sin\gamma_1 & 0 \\ -\sin\gamma_1 & \cos\gamma_1 & 0 \\ 0 & 0 & 1 \end{bmatrix} \begin{bmatrix} \cos\beta_1 & 0 & -\sin\beta_1 \\ 0 & 1 & 0 \\ \sin\beta_1 & 0 & \cos\beta_1 \end{bmatrix} \begin{bmatrix} \cos\alpha_1 & \sin\alpha_1 & 0 \\ -\sin\alpha_1 & \cos\alpha_1 & 0 \\ 0 & 0 & 1 \end{bmatrix}$$

$$= \begin{bmatrix} \cos\alpha_1\cos\beta_1\cos\gamma_1 - \sin\alpha_1\sin\gamma_1 & \sin\alpha_1\cos\beta_1\cos\gamma_1 + \cos\alpha_1\sin\alpha\gamma_1 & -\sin\beta_1\cos\gamma_1 \\ -\cos\alpha_1\cos\beta_1\sin\gamma_1 - \sin\alpha_1\cos\gamma_1 & -\sin\alpha_1\cos\beta_1\sin\gamma_1 + \cos\alpha_1\cos\gamma_1 & \sin\beta_1\sin\gamma_1 \\ \cos\alpha_1\sin\beta_1 & \sin\alpha_1\sin\beta_1 & \cos\beta_1 \end{bmatrix} \tag{A.1}$$

For molecule 2, the relation between the Euler angles and direction cosines is given by

$$l_{i'}^{\alpha} = \begin{bmatrix} \cos\gamma_2 & \sin\gamma_2 & 0 \\ -\sin\gamma_2 & \cos\gamma_2 & 0 \\ 0 & 0 & 1 \end{bmatrix} \begin{bmatrix} \cos\beta_2 & 0 & -\sin\beta_2 \\ 0 & 1 & 0 \\ \sin\beta_2 & 0 & \cos\beta_2 \end{bmatrix} \begin{bmatrix} \cos\alpha_2 & \sin\alpha_2 & 0 \\ -\sin\alpha_2 & \cos\alpha_2 & 0 \\ 0 & 0 & 1 \end{bmatrix}$$

$$= \begin{bmatrix} \cos\alpha_2\cos\beta_2\cos\gamma_2 - \sin\alpha_2\sin\gamma_2 & \sin\alpha_2\cos\beta_2\cos\gamma_2 + \cos\alpha_2\sin\alpha\gamma_2 & -\sin\beta_2\cos\gamma_2 \\ -\cos\alpha_2\cos\beta_2\sin\gamma_2 - \sin\alpha_2\cos\gamma_2 & -\sin\alpha_2\cos\beta_2\sin\gamma_2 + \cos\alpha_2\cos\gamma_2 & \sin\beta_2\sin\gamma_2 \\ \cos\alpha_2\sin\beta_2 & \sin\alpha_2\sin\beta_2 & \cos\beta_2 \end{bmatrix} \tag{A.2}$$

where

$$\left\{ \begin{array}{c} 0 \leq \alpha \leq 2\pi \\ \\ 0 \leq \beta \leq \pi \\ \\ 0 \leq \gamma \leq 2\pi \end{array} \right\}. \tag{A.3}$$

The six Euler angle above, together with the R parameter (which gives the intermolecular separation), are sufficient to fully describe the relative configuration of the two interacting molecules.

The general form of the $T-$tensors is [2]

$$T^{(1)} = (-1)^n T^{(2)} \tag{A.4}$$

where n is the order of the $T-$tensor. The second-rank $T-$tensor is given as

$$T^{(1)}_{\alpha\beta} = \frac{1}{4\pi\varepsilon_0}\nabla_\alpha\nabla_\beta R^{-1} = \frac{1}{4\pi\varepsilon_0}(3R_\alpha R_\beta - R^2\delta_{\alpha\beta})R^{-5} \tag{A.5}$$

where R is the relative separation of the interacting molecules measured from their respective origin. The third-rank $T-$tensor is given as

$$T^{(1)}_{\alpha\beta\gamma} = -\frac{1}{4\pi\varepsilon_0}\nabla_\alpha\nabla_\beta\nabla_\gamma R^{-1} = \frac{3}{4\pi\varepsilon_0}[5R_\alpha R_\beta R_\gamma - R^2(R_\alpha\delta_{\beta\gamma} + R_\beta\delta_{\gamma\alpha} + R_\gamma\delta_{\alpha\beta})]R^{-7}. \tag{A.6}$$

[1] V. W. Couling, PhD thesis, Second light-scattering and Kerr-effect virial coeffcients of molecules with linear and lower symmetry, University of Natal (1995).

[2] A. D. Buckingham, Permanent and induced molecular moments and long-range intermolecular forces, *Adv. Chem. Phys.*, **12**, 107-142 (1967).

A.2 The Total Oscillating Dipole of Molecule 1 in the presence of Molecule 2

The total induced electric-dipole moment of a representative molecule 1 in terms of molecular-property tensors is given below [1]. The inducing electric field is that of the light beam ξ_{0i} as well as the field due to the oscillating dipole moment of the neighbouring molecule 2.

$$\begin{aligned}
\mu_i^{(1)}(\xi_0) = {} & \alpha_{ij}^{(1)}\xi_{0j} + \alpha_{ij}^{(1)}T_{jk}\alpha_{kl}^{(2)}\xi_{0l} + \alpha_{ij}^{(1)}T_{jk}\alpha_{kl}^{(2)}T_{lm}\alpha_{mn}^{(1)}\xi_{0n} + \alpha_{ij}^{(1)}T_{jk}\alpha_{kl}^{(2)}T_{lm}\alpha_{mn}^{(1)}T_{nw}\alpha_{wv}^{(2)}\xi_{0v} + ... \\
& + \beta_{ijk}^{(1)}E_j\xi_{0k} + \beta_{ijk}^{(1)}E_jT_{km}\alpha_{mn}^{(2)}\xi_{0n} + \beta_{ijk}^{(1)}E_jT_{km}\alpha_{mn}^{(2)}T_{nw}\alpha_{wv}^{(1)}\xi_{0v} \\
& + \beta_{ijk}^{(1)}E_jT_{km}\alpha_{mn}^{(2)}T_{nw}\alpha_{wv}^{(1)}T_{vp}\alpha_{ps}^{(2)}\xi_{0s} + \alpha_{ij}^{(1)}T_{jk}\beta_{kmn}^{(2)}E_m\xi_{0n} + \alpha_{ij}^{(1)}T_{jk}\beta_{kmn}^{(2)}E_mT_{nw}\alpha_{wv}^{(1)}\xi_{0v} \\
& + \alpha_{ij}^{(1)}T_{jk}\alpha_{kl}^{(2)}T_{lm}\beta_{mnw}^{(1)}E_n\xi_{0w} + \alpha_{ij}^{(1)}T_{jk}\alpha_{kl}^{(2)}T_{lm}\alpha_{mn}^{(1)}T_{nw}\beta_{wvp}^{(2)}E_v\xi_{0p} \\
& + \alpha_{ij}^{(1)}T_{jk}\alpha_{kl}^{(2)}T_{lm}\beta_{mnw}^{(1)}E_nT_{wv}\alpha_{vp}^{(2)}\xi_{0p} + \alpha_{ij}^{(1)}T_{jk}\beta_{klm}^{(2)}E_mT_{ln}\alpha_{nw}^{(1)}T_{wv}\alpha_{vp}^{(2)}\xi_{0p} + ... \\
& + \frac{1}{2}\gamma_{ijkl}^{(1)}E_kE_l\xi_{0j} + \frac{1}{2}\gamma_{ijkl}^{(1)}E_kE_lT_{jm}\alpha_{mn}^{(2)}\xi_{0n} + \frac{1}{2}\gamma_{ijkl}^{(1)}E_kE_lT_{jm}\alpha_{mn}^{(2)}T_{nw}\alpha_{wv}^{(1)}\xi_{0v} \\
& + \frac{1}{2}\gamma_{ijkl}^{(1)}E_kE_lT_{jm}\alpha_{mn}^{(2)}T_{nw}\alpha_{wv}^{(1)}T_{vp}\alpha_{ps}^{(2)}\xi_{0s} + \frac{1}{2}\alpha_{ij}^{(1)}T_{jk}\gamma_{klmn}^{(2)}E_lE_m\xi_{0n} \\
& + \frac{1}{2}\alpha_{ij}^{(1)}T_{jk}\gamma_{klmn}^{(2)}E_lE_mT_{nw}\alpha_{wv}^{(1)}\xi_{0v} + \frac{1}{2}\alpha_{ij}^{(1)}T_{jk}\alpha_{kl}^{(2)}T_{lm}\gamma_{mnwv}^{(1)}E_nE_w\xi_{0v} \\
& + \frac{1}{2}\alpha_{ij}^{(1)}T_{jk}\alpha_{kl}^{(2)}T_{lm}\alpha_{mn}^{(1)}T_{nw}\gamma_{wvps}^{(2)}E_pE_s\xi_{0v} + \frac{1}{2}\alpha_{ij}^{(1)}T_{jk}\alpha_{kl}^{(2)}T_{lm}\gamma_{mnwv}^{(1)}E_nE_wT_{vp}\alpha_{ps}^{(2)}\xi_{0s} \\
& + \frac{1}{2}\alpha_{ij}^{(1)}T_{jk}\gamma_{klmn}^{(2)}E_nE_mT_{lw}\alpha_{wv}^{(1)}T_{vp}\alpha_{ps}^{(2)}\xi_{0s} + ...
\end{aligned} \tag{A.7}$$

The differential polarizability of molecule 1 in the presence of both the applied static field and a neighbouring molecule 2 is given as $\pi_{ij}^{(1)} = \frac{\partial \mu_i^{(1)}}{\xi_{0j}}$ which, together with the above expression, yields

$$
\begin{aligned}
\pi_{ij}^{(1)} = {} & \alpha_{ij}^{(1)} + \alpha_{ik}^{(1)} T_{kl} \alpha_{lj}^{(2)} + \alpha_{ik}^{(1)} T_{kl} \alpha_{lm}^{(2)} T_{mn} \alpha_{nj}^{(1)} + \alpha_{ik}^{(1)} T_{kl} \alpha_{lm}^{(2)} T_{mn} \alpha_{nw}^{(1)} T_{wv} \alpha_{vj}^{(2)} + ... \\
& + \beta_{ijk}^{(1)} E_k + \beta_{ikl}^{(1)} E_k T_{lm} \alpha_{mj}^{(2)} + \alpha_{ik}^{(1)} T_{kl} \beta_{lmj}^{(2)} E_m + \beta_{ikl}^{(1)} E_k T_{lm} \alpha_{mn}^{(2)} T_{nw} \alpha_{wk}^{(1)} \\
& + \alpha_{ik}^{(1)} T_{kl} \beta_{lmn}^{(1)} E_m T_{mv} \alpha_{vj}^{(2)} + \alpha_{ik}^{(1)} T_{kl} \alpha_{lm}^{(2)} T_{mn} \beta_{nwj}^{(1)} E_w + \beta_{ikl}^{(1)} E_k T_{lm} \alpha_{mn}^{(2)} T_{nw} \alpha_{wv}^{(1)} T_{vp} \alpha_{pj}^{(2)} \\
& + \alpha_{ik}^{(1)} T_{kl} \alpha_{lm}^{(2)} T_{mn} \alpha_{nw}^{(1)} T_{wv} \beta_{vjp}^{(2)} E_p + \alpha_{ik}^{(1)} T_{kl} \alpha_{lm}^{(2)} T_{mn} \beta_{nwv}^{(1)} E_v T_{wp} \alpha_{pj}^{(2)} \\
& + \alpha_{ik}^{(1)} T_{kl} \beta_{lmn}^{(2)} E_m T_{wv} \alpha_{nw}^{(1)} T_{vp} \alpha_{pj}^{(2)} + ... \\
& + \frac{1}{2} \gamma_{ijkl}^{(1)} E_k E_l + \frac{1}{2} \gamma_{iklm}^{(1)} E_m E_l T_{km} \alpha_{mj}^{(2)} + \frac{1}{2} \alpha_{ik}^{(1)} T_{kl} \gamma_{jlmn}^{(1)} E_m E_n \\
& + \frac{1}{2} \gamma_{iklm}^{(1)} E_k E_l T_{mn} \alpha_{nw}^{(2)} T_{wv} \alpha_{vj}^{(1)} + \frac{1}{2} \alpha_{ik}^{(1)} T_{kl} \gamma_{lmnw}^{(2)} E_w E_n T_{mv} \alpha_{vj}^{(1)} \\
& + \frac{1}{2} \alpha_{ik}^{(1)} T_{kl} \alpha_{lm}^{(2)} T_{mn} \gamma_{jnwv}^{(1)} E_w E_v + \frac{1}{2} \gamma_{iklm}^{(1)} E_k E_l T_{mn} \alpha_{nw}^{(2)} T_{wv} \alpha_{vp}^{(1)} T_{ps} \alpha_{sj}^{(2)} \\
& + \frac{1}{2} \alpha_{ik}^{(1)} T_{kl} \alpha_{lm}^{(2)} T_{mn} \alpha_{nw}^{(1)} T_{wv} \gamma_{jvps}^{(2)} E_p E_s + \frac{1}{2} \alpha_{ik}^{(1)} T_{kl} \alpha_{ml}^{(2)} T_{mn} \gamma_{nwvp}^{(1)} E_p E_v T_{ws} \alpha_{sj}^{(2)} \\
& + \frac{1}{2} \alpha_{ik}^{(1)} T_{kl} \gamma_{lmnw}^{(2)} E_w E_n T_{mv} \alpha_{vp}^{(1)} T_{ps} \alpha_{sj}^{(2)} + ...
\end{aligned}
\tag{A.8}
$$

The expressions for both the total induced dipole moment and the differential polarizability of molecule 2 are similar to that of molecule 1, with superscripts 1 and 2 being interchanged.

[1] V. W. Couling, PhD thesis, Second light-scattering and Kerr-effect virial coeffcients of molecules with linear and lower symmetry, University of Natal (1995).

A.3 The Potential Energy of a Representative Molecule p.

The potential energy of an interacting molecule p under the influence of static electric field E_i may be written as [1]

$$\begin{aligned} U^{(1)}(\tau, E) = &-(\mu(p)_{0i} + \alpha_{ij}^{(p)} T_{jk} \mu_{0k}^{(q)} + \alpha_{ij}^{(p)} T_{jk} \alpha_{kl}^{(q)} T_{lm} \mu_{0m}^{(q)} + \alpha_{ij}^{(p)} T_{jk} \alpha_{kl}^{(q)} T_{lm} \alpha_{mn}^{(p)} T_{nw} \mu_{0w}^{(q)} + ...) E l_i^x \\ &- \frac{1}{2}(\alpha_{ij}^{(p)} + \alpha_{ik}^{(p)} T_{kl} \alpha_{lj}^{(q)} + \alpha_{ik}^{(p)} T_{kl} \alpha_{lm}^{(q)} T_{mn} \alpha_{nj}^{(p)} + \alpha_{ik}^{(p)} T_{kl} \alpha_{lm}^{(q)} T_{mn} \alpha_{nw}^{(p)} T_{wv} \alpha_{vj}^{(q)} + ...) E^2 l_i^x l_j^x \\ &- O(E^3) - ... \end{aligned} \tag{A.9}$$

where $E l_i^x$ is written in place of E_i

[1] V. W. Couling, PhD thesis, Second light-scattering and Kerr-effect virial coeffcients of molecules with linear and lower symmetry, University of Natal (1995).

Appendix B

B.1 The HP-BASIC program used to run the experiment

```
10 REM ********************************************************
20 REM Program to control the Kerr-effect experiment        ****
30 REM Written 2013-2014 by Mzungezi Mthembu                ****
40 REM and by Vincent Couling                               ****
50 REM                                                      ****
60 REM                                                      ****
70 REM                                                      ****
80 REM Always set Prism min and max values +/- 0.5 degree   ****
90 REM MODIFIED for 0.5 degree analyzer offset              ****
100 REM Using the AG-PR100P rotation stage and the ...      ****
110 REM ... CONEX-P Agilis precision rotator controller     ****
111 REM                                                     ****
120 REM ********************************************************
130 COM Ve
140 CLEAR SCREEN
150 REM ********************************************************
160 REM Open communications with the CONEX-P Agilis controller ...
170 REM ... and rotate the prism to home
180 REM ********************************************************
190 ASSIGN @Devices TO 1
```

```
200 ASSIGN @Io_path TO 9
210 CONTROL 9,3;57600 ! set the BAUD rate to 57 000 bps
220 OUTPUT 9;"1VE"
230 PRINT "Check VE version ... "
240 ENTER 9;Ve$
250 WAIT 1
260 PRINT "1VE = ";Ve$
270 PRINT "Finding home ... "
280 OUTPUT 9;"1OR" ! Execute home search
290 PRINT "Wait 30 seconds ... "
300 WAIT 3
310 REM **************************
320 REM File names for data storage
330 REM **************************
340 Efgibfile1$="7Oct2014-1Kerr"
350 Tempfile1$="7Oct2014-1Ktemp"
360 Currentfile1$="7Oct2014-1Kcurr"
370 Datafile1$="7Oct2014-1Kdata"
380 PRINTER IS CRT ! The variables are declared in statements below.
390 REM ************************
400 REM declare common variables
410 REM ************************
420 COM I,Counter1,No1,Sig1,T,Temp45(1000),Preset(1000),Pg,Pa,Psd(25),Iac(25)
    ,Hvac(25)
430 COM Hv(15),M(1000),C(1000),R(1000),Nulli(1000),Hiv(1000),Ctime(3200),
    Counting
431 COM M_2(1000),C_2(1000),R_2(1000),Nulli_2(1000)
440 COM Switch(3200),W,V,Counterp1,Counterp2,Diff,Err45,Err4tsp,Pid_dl
450 COM Acumsec2(3200),Ferrlast,Ferr1,Time3,Time4,Time5,Difftime,Counter2,Vtot
460 COM Efgibfile$[40],Tempfile$[40],Presfile$[40],Warning$[80]
470 COM Highvolts,Ni,Err1(3200),Err2(3200),Err3(3200),Err4(3200),Temperature
480 COM Err5(3200),C02,Int1(3200),Closetime(3200),Scaledtime,Voltage1,Voltage2,
```

```
    Temp45a(1000)
490 COM Temp45b(1000),Temp45c(1000),Param,Volta,Voltb,Zz(1000),Press(1000),Pre
500 COM Param1,Param2,Param3!,Param4
510 COM Prism_min,Prism_max,Res,Iac_2(25)
511 !COM Prism_min1$,Prism_max1$
520 Scaledtime=0
530 Ni=1
540 REM ************************************************************************
550 REM Establish the analyzer offsets using CONEX.BAS, then modify accordingly ...
560 REM ... for the max and min limits below:
570 REM ************************************************************************
580 Prism_min=171.350!80.83! These two values should differ by 1 degree
581 PRINT "Prism min ";Prism_min
590 Prism_max=172.350!80.83! so that the offset is +/- 0.5 of a degree
591 PRINT "Prism max ";Prism_max
600 Prism_min$="171.350" ! converts the value to a string
610 Prism_max$="172.350"
620 PRINT "Prism rotating to maximum position of ",Prism_max," degrees ... "
630 OUTPUT 9;"1PA"&Prism_max$
640 PRINT "Wait 30 seconds ... "
650 WAIT 30
660 REM ******************************
670 REM Open the files for data storage
680 REM ******************************
690 CREATE Efgibfile1$,1
700 CREATE Tempfile1$,1
710 CREATE Currentfile1$,1
720 CREATE Datafile1$,1
730 ASSIGN @File TO Efgibfile1$;APPEND
740 ASSIGN @File TO Tempfile1$;APPEND
750 ASSIGN @File TO Currentfile1$;APPEND
760 ASSIGN @File TO Datafile1$;APPEND
```

```
770 PRINT "Please enter gas name" !User inputs the name of the gas.
780 INPUT Gasname$
790 PRINT "please enter gas pressure (MPa)" !User inputs the pressure.
800 INPUT Pg
810 PRINT "please enter PSD time constant" ! ususally 1 sec
820 INPUT Param$
830 PRINT "please enter PSD sensitivity" ! ? micro Volts
840 INPUT Param1$
850 PRINT "please enter type of Faraday Cell" ! Water, toluene, glass?
860 INPUT Param2$
870 PRINT "please enter Faraday Cell current-limiting resistance" ! to limit the
    Faraday Cell current
880 INPUT Param3$
885 Res=1995.3!5257.7!5258.8!10051.9!5231.4!2613.9 !1005.67
    ! The 4-wire R value to confirm the ac Faraday Cell current
890 CLEAR SCREEN
900 PRINTER IS Efgibfile1$;APPEND
910 PRINT "Measurement of molecular quadrupole moment for ";Gasname$
920 PRINT "Time is ";TIME$(TIMEDATE)
930 PRINT "Date is ";DATE$(TIMEDATE)
940 PRINT "Cell pressure (gauge) in  MPa ";Pg
950 PRINT "PSD time constant  ";Param$
960 PRINT "PSD sensitivity  ";Param1$
970 PRINT "Type of Faraday Cell  ";Param2$
980 PRINT "Faraday Cell current-limiting resistance  ";Param3$
990 PRINT "Maximum analyzer offset is (degrees)  ";Prism_max
1000 PRINT "Minimum analyzer offset is (degrees)  ";Prism_min
1010 PRINTER IS CRT
1020 Counter1=1
1030 No1=0
1040 Sig1=1
1050 ON KEY 6 LABEL "Terminate" GOTO 3060
```

```
1060 REM ******************************
1070 REM reset and initialize Agilent DAU
1080 REM ******************************
1090 OUTPUT 710;"*rst"       !Reset data acquisition unit to factory settings.
1100 OUTPUT 710;"*cls"
1110 PRINT "SWITCH ON HV, AND PRESS ENTER"
1120 ON KBD GOTO 1130
1130 OUTPUT 710;"rout:scan(@103,104,105,106,107,108,109,112,113,122)"
1140 CLEAR SCREEN
1150 PRINTER IS Efgibfile1$;APPEND
1160 Highvolts=0
1170 ounting=0
1180 OUTPUT 710;"route:close (@201)"  !Reset the current attenuator to zero
1190 OUTPUT 710;"route:open (@201)"
1200 OUTPUT 710;"route:close (@203)"   !Transfer to reset counter to zero
1210 OUTPUT 710;"route:close (@203)"
1220 Temperature=0
1230 FOR Z=0 TO 9 !Do loop for taking 10 measurments.
1240 FOR I=0 TO 50  !Do loop to vary current through FC and change phase.
1250 OUTPUT 710;"route:close (@202)"  !count 50 times then change current ic FC
1260 OUTPUT 710;"route:open (@202)"
1270 !Counting=Counting+I
1280 NEXT I
1290 !PRINT "i = ",I
1300 Counting=Counting+I
1310 !PRINT "Counting = ",Counting
1320 OUTPUT 710;"route:close (@203)" !Data transfer occurs at this point.
1330 OUTPUT 710;"route:close (@203)"
1340 WAIT 5
1350 OUTPUT 710;"conf:curr:ac (@122)"  !Read the current in FC
1360 OUTPUT 710;"read?"
1370 ENTER 710;Iac(Z+1)
```

```
1371 OUTPUT 710;"conf:volt:ac (@112)"  !Read the voltage across the FC resistor
1372 OUTPUT 710;"read?"
1373 ENTER 710;Iac_2(Z+1)
1374 Iac_2(Z+1)=Iac_2(Z+1)/Res
1380 IF Counting>256 THEN Iac(Z+1)=-1*Iac(Z+1) !Manually change current phase
1382 IF Counting>256 THEN Iac_2(Z+1)=-1*Iac_2(Z+1) !Manually change current phase
1390 PRINTER IS CRT
1391 OUTPUT 710;"conf:volt:dc (@113)"  !Read the Pressure Transducer voltage
1392 OUTPUT 710;"read?"
1393 ENTER 710;Press(Z+1)
1400 !WAIT 5
1410 !OUTPUT 710;"conf:temp TC,J,(@101)" !Measure the room temperature using a
     J-type thermocouple
1420 !OUTPUT 710;"read?"
1430 !OUTPUT 710;"read?"
1440 !ENTER 710;Temp45(Z+1)
1450 OUTPUT 710;"conf:temp FRTD,85,(@108)" !Measure the cell temperature using
     a PT100, 4-wire
1460 OUTPUT 710;"read?"
1470 ENTER 710;Temp45a(Z+1)
1480 !Temp45(Z+1)=Temp45(Z+1)
1481 !Temp45a(Z+1)=Temp45(Z+1)
1490 OUTPUT 710;"conf:temp FRTD,85,(@109)" !Measure the cell temperature using
     a PT100
1500 OUTPUT 710;"read?"
1510 ENTER 710;Temp45b(Z+1)
1520 !Temp45b(Z+1)=Temp45(Z+1)
1530 !OUTPUT 710;"conf:temp FRTD,85,(@107)" !Measure the cell temperature using
     a PT100
1540 !OUTPUT 710;"read?"
1550 !ENTER 710;Temp45c(Z+1)
1560 !Temp45c(Z+1)=Temp45(Z+1)
```

```
1570 !WAIT 6
1580 GOSUB 1970 !Take 20 psd reading and average
1590 !OUTPUT 709;"conf:volt:dc (@103)" !Measure psd voltages
1600 !OUTPUT 709;"read?"
1610 !ENTER 709;Psd(Z+1)
1620 PRINTER IS Efgibfile1$;APPEND
1630 !PRINT "Voltage =";Psd(Z+1);"Current is ";Iac(Z+1) !Measure current in FC.
1640 OUTPUT 710;"conf:volt:dc (@104)" !Measure HV transformer voltage
1650 OUTPUT 710;"read?"
1660 ENTER 710;Hvac(Z+1)
1670 Highvolts=Highvolts+Hvac(Z+1)
1680 !Temperature=Temperature+(Temp45a(Z+1)+Temp45b(Z+1)+Temp45c(Z+1))/3
     !average cell temperature
1681 Temperature=Temperature+(Temp45a(Z+1)+Temp45b(Z+1))/2
     !average cell temperature
1690 PRINT "Voltage = ";Psd(Z+1);"Current is ";Iac(Z+1),"Hv is
     ";Hvac(Z+1);Counting;Temp45a(Z+1);Temp45b(Z+1);(Temp45a(Z+1)+Temp45b(Z+1))/2
1691 PRINT "Voltage = ";Psd(Z+1);"C_2 is ";Iac_2(Z+1),"Hv is
     ";Hvac(Z+1);Counting;Temp45a(Z+1);Temp45b(Z+1);(Temp45a(Z+1)+Temp45b(Z+1))/2
1692 PRINT "Pressure = ";Press(Z+1)*1503.999-1410.95
1693 Pre=Press(Z+1)*1503.999-1410.95 !HV calibration 5 August 2014
1700 PRINTER IS CRT ! _2 is FC measured via V and R
1710 PRINT "Voltage = ";Psd(Z+1);"Current is ";Iac(Z+1),"Hv is
     ";Hvac(Z+1);Counting;Temp45a(Z+1);Temp45b(Z+1);(Temp45a(Z+1)+Temp45b(Z+1))/2
1711 PRINT "Voltage = ";Psd(Z+1);"C_2 is ";Iac_2(Z+1),"Hv is
     ";Hvac(Z+1);Counting;Temp45a(Z+1);Temp45b(Z+1);(Temp45a(Z+1)+Temp45b(Z+1))/2
1712 PRINT "Pressure = ";Press(Z+1)*1503.999-1410.95
1720 NEXT Z
1730 PRINT "the average high voltage to the cell is ";Highvolts/10
1740 GOSUB 2120  !perform linear regression after each run
1750 PRINTER IS Efgibfile1$;APPEND
1760 Ni=Ni*(-1)
```

```
1770 REM ************************************************************
1780 REM Subroutine used to rotate stepper motor and hence the analyzer
         to desired value.
1790 REM ************************************************************
1800 IF Ni=1 THEN GOTO 1820
1810 IF Ni=-1 THEN GOTO 1860
1820 OUTPUT 9;"1PA"&Prism_max$
1830 WAIT 15
1840 PRINT "rotated forward ... "
1850 GOTO 1140
1860 OUTPUT 9;"1PA"&Prism_min$
1870 WAIT 15
1880 PRINT "rotated backwards ... "
1890 GOTO 1140
1900 REM ***************************
1910 REM ***************************
1920 PRINT "end"
1930 PRINT "end"
1940 !GOTO 4100 !Compute mQ
1950 REM
1960 REM
1970 REM ************************************************************
1980 REM The subroutine to take 20 psd readings and calculate it average
1990 REM ************************************************************
2000 OUTPUT 710;"conf:volt:dc (@103)" !Measure psd voltages
2010 Voltage1=0
2020 Voltage2=0
2030 WAIT 5
2040 FOR Ii=1 TO 20
2050 OUTPUT 710;"read?"
2060 ENTER 710;Voltage1
2070 Voltage2=Voltage2+Voltage1
```

```
2080 WAIT 1/2
2090 NEXT Ii
2100 Psd(Z+1)=Voltage2/20
2110 RETURN
2120 REM ******************************************
2130 REM The subroutine to perform linear regression
2140 REM ******************************************
2150 REM
2160 No1=No1+1
2170 X=0
2171 X_2=0
2180 Xy=0
2181 Xy_2=0
2190 Y=0
2200 X2=0
2201 X2_2=0
2210 Y2=0
2220 Zz(No1)=Psd(10)
2230 FOR Ij=1 TO 10
2240 Y=Y+Psd(Ij)
2250 X=X+Iac(Ij)
2251 X_2=X_2+Iac_2(Ij)
2260 Xy=Xy+Iac(Ij)*Psd(Ij)
2261 Xy_2=Xy_2+Iac_2(Ij)*Psd(Ij)
2270 X2=X2+Iac(Ij)*Iac(Ij)
2271 X2_2=X2_2+Iac_2(Ij)*Iac_2(Ij)
2280 Y2=Y2+Psd(Ij)*Psd(Ij)
2290 NEXT Ij
2300 M(No1)=(10*Xy-X*Y)/(10*X2-X^2)
2301 M_2(No1)=(10*Xy_2-X_2*Y)/(10*X2_2-X_2^2)
2310 C(No1)=(Y*X2-X*Xy)/(10*X2-X^2)
2311 C_2(No1)=(Y*X2_2-X_2*Xy_2)/(10*X2_2-X_2^2)
```

```
2320 R(No1)=SQR((10*Xy-X*Y)^2/((10*X2-X^2)*(10*Y2-Y^2)))
2321 R_2(No1)=SQR((10*Xy_2-X_2*Y)^2/((10*X2_2-X_2^2)*(10*Y2-Y^2)))
2330 Hiv(No1)=Highvolts/10
2340 PRINTER IS Efgibfile1$;APPEND
2350 PRINT
2360 PRINT "slope = ";M(No1)/1000;"V/mA"
2361 PRINT "slope_2 = ";M_2(No1)/1000;"V/mA"
2370 PRINT "intercept = ";C(No1);"v"
2371 PRINT "intercept_2 = ";C_2(No1);"v"
2380 PRINT "r = ";R(No1)
2381 PRINT "r_2 = ";R_2(No1)
2390 PRINT "Zz(1) = ";Zz(1)
2400 PRINT
2410 PRINT
2420 PRINTER IS CRT
2430 PRINT "slope = ",M(No1)/1000;"v/mA"
2431 PRINT "slope_2 = ",M_2(No1)/1000;"v/mA"
2440 PRINT "intercept = ";C(No1);"V"
2441 PRINT "intercept_2 = ";C_2(No1);"V"
2450 PRINT "r = ";R(No1)
2451 PRINT "r_2 = ";R_2(No1)
2460 PRINT "Zz(1) = ";Zz(1)
2470 PRINT
2480 IF R(No1)<.995 THEN
2490 IF No1 MOD 2 THEN
2500 R(No1)=R(No1-1)
2501 R_2(No1)=R_2(No1-1)
2510 END IF
2520 No1=No1-1
2530 PRINT "bad run"
2540 GOTO 1160
2550 END IF
```

```
2560 IF Sig1=-1 THEN GOSUB 2600
2570 Sig1=-1*Sig1
2580 RETURN
2590 REM
2600 REM ******************************************
2610 REM The subroutine to determine the null current
2620 REM ******************************************
2630 REM
2640 Nulli(No1/2)=(C(No1)-C(No1-1))/(M(No1-1)-M(No1))
2641 Nulli_2(No1/2)=(C_2(No1)-C_2(No1-1))/(M_2(No1-1)-M_2(No1))
2650 Nullpsd=M(No1)*Nulli(No1/2)+C(No1)
2651 Nullpsd_2=M_2(No1)*Nulli_2(No1/2)+C_2(No1)
2660 PRINTER IS Efgibfile1$;APPEND
2670 PRINT
2680 PRINT "Run no ";No1/2
2690 PRINT "the null current is ";Nulli(No1/2)*1000;"mA"
2691 PRINT "the null current_2 is ";Nulli_2(No1/2)*1000;"mA"
2700 PRINT "the null voltage is ";Nullpsd;"V"
2701 PRINT "the null voltage_2 is ";Nullpsd_2;"V"
2710 PRINT " the correlation co-efficients were ";R(No1-1);" and";R(No1)
2711 PRINT " the correlation co-efficients_2 were ";R_2(No1-1);" and";R_2(No1)
2720 Temp45(No1/2)=FNTemperature
2730 PRINT Counter1;"room temp";Temperature/10;"pressure ";Pg;"time = "
     ;TIME$(TIMEDATE);"date";DATE$(TIMEDATE)
2740 PRINT "High voltage average ",Highvolts/10
2750 PRINT
2760 PRINT
2770 PRINTER IS Datafile1$;APPEND
2780 PRINT "Run no ";No1/2
2790 PRINT "the null current is ";Nulli(No1/2)*1000;"mA"
2791 PRINT "the null current_2 is ";Nulli_2(No1/2)*1000;"mA"
2800 PRINT "the null voltage is ";Nullpsd;"V"
```

```
2801 PRINT "the null voltage_2 is ";Nullpsd_2;"V"
2810 PRINT " the correlation co-efficients were ";R(No1-1);" and";R(No1)
2811 PRINT " the correlation co-efficients_2 were ";R_2(No1-1);" and";R_2(No1)
2820 PRINT "slope = ",M(No1)/1000;"v/mA"
2821 PRINT "slope_2 = ",M_2(No1)/1000;"v/mA"
2830 PRINT "intercept = ";C(No1);"V"
2831 PRINT "intercept_2 = ";C_2(No1);"V"
2840 !PRINTER IS CRT
2850 !Pres(No1/2)=Pg
2860 PRINT
2870 PRINT
2880 PRINTER IS CRT
2890 PRINT "Run no ";No1/2
2900 PRINT "the null current is ";Nulli(No1/2)*1000;"mA"
2901 PRINT "the null current_2 is ";Nulli_2(No1/2)*1000;"mA"
2910 PRINT "the null voltage is ";Nullpsd;"V"
2911 PRINT "the null voltage_2 is ";Nullpsd_2;"V"
2920 PRINT " the correlation co-efficients were ";R(No1-1);" and";R(No1)
2921 PRINT " the correlation co-efficients_2 were ";R_2(No1-1);" and";R_2(No1)
2930 PRINT Counter1;"room temp";Temperature/10;"pressure ";Pg;"time = ";
TIME$(TIMEDATE);"date = ";DATE$(TIMEDATE)
2940 PRINTER IS Currentfile1$;APPEND
2950 PRINT Nulli(No1/2)*1000;Nulli_2(No1/2)*1000;Temperature/10;Highvolts/10;Pre
2951 ! PRINT "Pressure = ";Press(Z+1)*1198.9885+101.1687
2960 PRINTER IS Tempfile1$;APPEND
2970 PRINT "Run no ";No1/2
2980 PRINT "the null current is ";Nulli(No1/2)*1000;"mA"
2981 PRINT "the null current_2 is ";Nulli_2(No1/2)*1000;"mA"
2990 PRINT "the null voltage is ";Nullpsd;"V"
2991 PRINT "the null voltage_2 is ";Nullpsd_2;"V"
3000  PRINT " the correlation co-efficients were ";R(No1-1);" and";R(No1)
3001 PRINT " the correlation co-efficients_2 were ";R_2(No1-1);" and";R_2(No1)
```

```
3010 PRINT Counter1;"cell temp";Temperature/10;"pressure ";Pg;"time = ";
TIME$(TIMEDATE);"date= ";DATE$(TIMEDATE)
3020 PRINT "High voltage average ",Highvolts/10
3030 PRINT
3040 PRINT
3050 RETURN
3060 END
3070 REM ************************************************
3080 REM The subfunction to determine the room temperature
3090 REM ************************************************
3100 DEF FNTemperature
3110 OUTPUT 710;"conf:temp TC,J,(@101)"
3120 OUTPUT 710;"read?"
3130 ENTER 710;Temp4
3140 RETURN Temp45
3150 Volta=Voltage1
3160 FNEND
```

B.2 The HP-BASIC program used to calibrate the Faraday cell

```
10 ! Program to automate calibration of the Water Faraday Cell
20 ! Written by Vincent Couling and Mzungezi Mthembu
30 ! 8 February 2013
40 ! Modified the FCCALIB5.BAS program for the Agilis Controller
50 ! Don't forget to load the 32-bit serial driver: Load Bin "serial32"
60 ! Uses RS232 port to control CONEX-P Agilis precision rotator controller
70 ! Driving the AG-PR100P rotation stage
80 ! Need a laser, polarizer, glass FC (ac current), water FC (dc current),
   analyzer and photodiode detector
90 COM Ja,Psd(12),Ang(12),Currentzero(12),Psdzero(12),M(30000),C(30000)
```

```
   ,R(30000),T
100 COM Order(12),Jj,Temp
110 Jj=1
120 Order(1)=1
130 Order(2)=10
140 Order(3)=2
150 Order(4)=9
160 Order(5)=3
170 Order(6)=8
180 Order(7)=4
190 Order(8)=7
200 Order(9)=5
210 Order(10)=6
220 ON KEY 6 LABEL "Terminate" GOTO 1920
230 CLEAR SCREEN
240 PRINT "INPUT PSD TIME CONSTANT"
250 INPUT T$
260 PRINT "INPUT PSD SENSITIVITY"
270 INPUT S$
271 PRINT "INPUT temperature deg C"
272 INPUT Temp
280 Fccalib1$="200214-FCcalib1a"
290 Fccalib2$="200214-FCcalib2a"
300 CREATE Fccalib1$,1
310 CREATE Fccalib2$,1
320 PRINTER IS Fccalib1$;APPEND
330 PRINT "Date is ";DATE$(TIMEDATE)
340 PRINT "Time is ";TIME$(TIMEDATE)
350 PRINT "Automated calibration of the water Faraday Cell ... "
360 PRINT "************************************************"
370 PRINT "     "
380 PRINT "PSD time constant is ",T$
```

```
390 PRINT "PSD sensitivity is ",S$
391 PRINT "temperature is ",Temp
400 PRINTER IS Fccalib2$;APPEND
410 PRINT "Date is ";DATE$(TIMEDATE)
420 PRINT "Time is ";TIME$(TIMEDATE)
421 PRINT "temperature is ",Temp
430 PRINT "Automated calibration of the water Faraday Cell ... "
440 PRINT "PSD time constant is ",T$
450 PRINT "PSD sensitivity is ",S$
451 PRINT "temperature is ",Temp
460 PRINT "Calibration constants in microradians per milliamp ... "
470 PRINTER IS CRT
480 ASSIGN @File TO Fccalib1$;APPEND
490 ASSIGN @File TO Fccalib2$;APPEND
500 ASSIGN @Devices TO 1
510 ASSIGN @Io_path TO 9
520 T=0
530 PRINT STATUS(9,3)
540 CONTROL 9,3;57600 ! set the baud rate to 57 600 bps
550 PRINT STATUS(9,3)
560 PRINT "Start ..."
570 OUTPUT 9;"1VE"
580 PRINT "Check VE version ..."
590 ENTER 9;Ja$
600 WAIT 1
610 PRINT "1VE = ",Ja$
620 PRINT "Finding home ..."
630 OUTPUT 9;"1OR" ! Execute home search
640 PRINT "Wait 30 seconds ..."
650 WAIT 30
660 Prism_min=123.06
670 Prism_max=124.36
```

```
680 Prism_min$=VAL$(Prism_min)
690 Prism_max$=VAL$(Prism_max)
700 PRINT "Prism rotating to minimum position of ",Prism_min,"degrees ..."
710 OUTPUT 9;"1PA"&Prism_min$
720 Ang(1)=Prism_min
730 PRINT "Wait 30 seconds ..."
740 WAIT 30
750 OUTPUT 705;"*rst,*cls" ! reset and configure dc power supply
760 OUTPUT 705;"appl p25v, 25.0, 0.0" ! set dc current to zero amps
770 OUTPUT 705;"outp on"
780 OUTPUT 722;"*rst,*cls" ! reset and configure the DMM to read dc current
790 OUTPUT 722;"conf:curr:dc"
800 Currentacc=0 ! set the accumulated current vaiable to zero
810 OUTPUT 709;"*rst" ! reset and configure the Data Acquisition Unit (DAU)
820 OUTPUT 709;"*cls"
830 OUTPUT 709;"rout:scan (@104)" ! channel 104 reads the PSD voltage
840 FOR N=1 TO 10 ! determines 10 equally-spaced current settings
850 Cur=Order(N)*.1 ! dc current ranges between 0.1 to 1.0 amps in 0.1 amp steps,
    staggered to avoid heating Faraday Cell
860 Cur$=VAL$(Cur) ! numerical value converted to a string
870 Currentacc=0 ! set the accumulated current variable to zero
880 WAIT 1
890 OUTPUT 705;"appl p25v, 25.0, ";Cur$ ! set dc current
900 OUTPUT 705;"outp on"
910 WAIT 5 ! pause for settling
920 FOR Prism=1 TO 10 ! determines 10 equally-spaced prism settings
930 Angle=Prism_min+(Prism_max-Prism_min)*(Prism-1)/9 !angle to rotate the prism to
940 Ang(Prism)=Angle
950 OUTPUT 9;"1PA"&VAL$(Angle)
960 PRINTER IS Fccalib1$;APPEND
970 PRINT "Prism Setting = ",Angle," degrees"
980 PRINTER IS CRT
```

```
990 PRINT "Prism Setting = ",Angle," degrees"
1000 WAIT 10
1010 OUTPUT 722;"measure:curr:dc?"! measure the dc current
1020 ENTER 722;Ct
1030 Currentacc=Currentacc+Ct! update the accumulated current variable
1040 OUTPUT 709;"conf:volt:dc (@104)"! configure the DAU channel 104 to read
     the PSD dc Volts
1050 V=0! current voltage variable
1060 Vtot=0! accumulated voltage variable
1070 FOR Ii=1 TO 20! accumulate 20 PSD voltage readings
1080 OUTPUT 709;"read?"! read the current voltage
1090 ENTER 709;V
1100 Vtot=Vtot+V! accumulate the voltage readings
1110 WAIT 1/10
1120 NEXT Ii
1130 Vtot=Vtot/20! determine the average PSD voltage for this current/
     prism setting
1140 PRINTER IS Fccalib1$;APPEND
1150 PRINT "Vtot ",Prism," = ",Vtot
1160 PRINTER IS CRT
1170 PRINT "Vtot ",Prism," = ",Vtot
1180 Psd(Prism)=Vtot! store the average PSD voltage in an array
1190 NEXT Prism
1200 Currentzero(N)=Currentacc/10
1210 REM linear regression
1220 X=0
1230 Xy=0
1240 Y=0
1250 X2=0
1260 Y2=0
1270 FOR Ij=1 TO 10
1280 Y=Y+Psd(Ij)
```

```
1290 X=X+Ang(Ij)
1300 Xy=Xy+Ang(Ij)*Psd(Ij)
1310 X2=X2+Ang(Ij)*Ang(Ij)
1320 Y2=Y2+Psd(Ij)*Psd(Ij)
1330 NEXT Ij
1340 M(N)=(10*Xy-X*Y)/(10*X2-X^2)
1350 C(N)=(Y*X2-X*Xy)/(10*X2-X^2)
1360 R(N)=SQR((10*Xy-X*Y)^2/((10*X2-X^2)*(10*Y2-Y^2)))
1370 PRINTER IS Fccalib1$;APPEND
1380 PRINT "Psd Voltage versus Rotational Angle for a current of "&Cur$&" Amps"
1390 PRINT "m = ",M(N)
1400 PRINT "c = ",C(N)
1410 PRINT "r = ",R(N)
1420 PRINTER IS CRT
1430 PRINT "Psd Voltage versus Rotational Angle for a current of "&Cur$&" Amps"
1440 PRINT "m = ",M(N)
1450 PRINT "c = ",C(N)
1460 PRINT "r = ",R(N)
1470 Psdzero(N)=-C(N)/M(N)
1480 WAIT 15
1490 NEXT N
1500 FOR N=1 TO 10
1510 PRINTER IS Fccalib1$;APPEND
1520 PRINT "psdzero ",N,Psdzero(N)," curr ",Currentzero(N)
1530 PRINTER IS CRT
1540 PRINT "psdzero ",N,Psdzero(N)," curr ",Currentzero(N)
1550 NEXT N
1560 X=0
1570 Xy=0
1580 Y=0
1590 X2=0
1600 Y2=0
```

```
1610 FOR N=1 TO 10
1620 Y=Y+Psdzero(N)
1630 X=X+Currentzero(N)
1640 Xy=Xy+Currentzero(N)*Psdzero(N)
1650 X2=X2+Currentzero(N)*Currentzero(N)
1660 Y2=Y2+Psdzero(N)*Psdzero(N)
1670 NEXT N
1680 M(Jj)=(10*Xy-X*Y)/(10*X2-X^2)
1690 C(Jj)=(Y*X2-X*Xy)/(10*X2-X^2)
1700 R(Jj)=SQR((10*Xy-X*Y)^2/((10*X2-X^2)*(10*Y2-Y^2)))
1710 !OUTPUT 709;"conf:temp FRTD,85,(@106)" ! measure room temp
1720 !OUTPUT 709;"read?"
1730 !ENTER 709;Temp
1740 PRINTER IS Fccalib1$;APPEND
1750 PRINT "Plot of Angle for Psd Null versus DC current in Faraday Cell for run
     number ",Jj
1760 PRINT "m = ",M(Jj)
1770 PRINT "c = ",C(Jj)
1780 PRINT "r = ",R(Jj)
1790 PRINT "Calibration constant of water Faraday cell is
     ",M(Jj)*2*3.14159265/360/1000," rad per mA"
1800 PRINT "Temperature of lab is ",Temp," degrees C"
1810 PRINTER IS Fccalib2$;APPEND
1820 PRINT M(Jj)*2*3.14159265/360*1000
1830 PRINTER IS CRT
1840 PRINT "Plot of Angle for Psd Null versus DC current in Faraday Cell for run
     number ",Jj
1850 PRINT "m = ",M(Jj)
1860 PRINT "c = ",C(Jj)
1870 PRINT "r = ",R(Jj)
1880 PRINT "Calibration constant of water Faraday cell is
     ",M(Jj)*2*3.14159265/360/1000," rad per mA"
```

```
1890 PRINT "Temperature of lab is ",Temp," degrees C"
1900 Jj=Jj+1
1910 GOTO 840
1920 END
```

B.3 The FORTRAN90 program used to calculate γ^K

```
module precision
implicit none
integer, parameter::rp=selected_real_kind(15)
end module precision


Program virial
use precision
Implicit none

! Program to calculate the molar Kerr constant mK
! Modified 20 June 2014 for He (from Ar)
! By Vincent Couling and Mzungezi Mthembu


real :: Temp,P,Bt,Ct,Vmideal,Vmnew,Vmold
real :: a,b,c,d,r,l,epsilon,lambda,t,q,Ex,er,n
real :: tdash,voltage,Pi,pressure,Patm,a1,a2,twod1,twod2,twod3,twod
real :: a3,a4,GAMMA_K,current,currerror,k,Na,Fcellcalib
real(rp)::bmQ,bmQne_r
real(rp)::delalpha,theta1,theta2,theta,theta1ne_r,theta2ne_r,thetane_r,bk,AE,BE
integer :: i
open(10,file="6Oct2014_Kerr1.dat")
```

```
write(*,*)"Enter the temperature in degrees Celsius"
read(*,*)Temp

write(*,*)"Enter the cell gauge pressure in MPa"
read(*,*)pressure

!write(*,*)"Enter atmospheric pressure in mmHg"
!read(*,*)Patm

write(*,*)"Enter the cell high voltage (dc scale)"
read(*,*)voltage

write(*,*)"Enter the average null current in mA"
read(*,*)current

write(*,*)"Enter the average null current uncertainty in mA"
read(*,*)currerror

write(*,*)"Enter the average electrode spacing in mm "
read(*,*)twod


pressure=pressure*10**6
voltage=voltage*991.57115+3.17487!correcting for HV calibration
Temp = Temp+273.15

pi=3.141592653589793
P = pressure!+(Patm/760.0)*101325.0
Bt = (9.2479 + 1087.6/Temp - 108800/Temp**2 + 2386900/Temp**3)/1000000
Ct = 102.5e-12!323K to 400K !1160.0e-12!Av at 295.0 K
k = 1.38065051e-23
!epsilon = 8.854187817e-12
```

```
Na = 6.0221415e23
!delalpha=1.223e-40_rp
ae=0.5172539e-6_rp !Ar 33 deg C
b=-0.06e-6!be=b*ae
c=-1.75e-12


write(*,*)'10^6  B = ',Bt*1.0e6,' m^3 mol^-1'
write(*,*)'10^12 C = ',Ct*1.0e12,' m^6 Mol^-2'
write(*,*)'P = ',P,' Pa'

Vmideal = 8.314472*Temp/P
Vmold = Vmideal
Vmnew = Vmideal*(1.+Bt/Vmold+Ct/Vmold**2)
i=1

   Do While (SQRT((Vmnew-Vmold)**2)>0.00000001)
   i=i+1
   Vmold=Vmnew
   Vmnew = Vmideal*(1.+Bt/Vmold+Ct/Vmold**2)
   End Do

l = 1.47543*1.001768
d=3.108e-3
epsilon=8.854187817e-12
voltage=voltage*SQRT(2.0)!*1.0051413833
Ex = voltage/d

er=(1.+2.*(ae*(1.+b/vmnew+c/vmnew**2)))/(1.-ae*(1.+b/vmnew+c/vmnew**2))
n=(34.808*2.2260956e-2/vmnew)*1.0e-6+1.0

!*********************************************************************!
```

```
!The following piece of code will calculate the molar Kerr constant!
!and finally the Kerr second Hyperpolarizability of the molecule.              !
!*****************************************************************************!
Fcellcalib=0.6228e-6
a1=current*Fcellcalib*Sqrt(2.)!174.5e-8*Sqrt(2.)!173e-8*Sqrt(2.)
a2=a1*81*epsilon/Na
a3=a2*632.8e-9/Pi/l
a4=a3*18.*n/(3*(n**2+2)**2*(er+2)**2)*((Vmnew)/(Ex**2))!*Sqrt(2.)
GAMMA_K=2.0*a4!factor of 2 from V**2     *epsilonr

write(*,*)'Gamma_K = ',GAMMA_K


!*****************************************************************************!
!The relevant pieces of information are written                                !
!to the screen and to a data file.                                             !
!*****************************************************************************!


write(*,*)'Vm iterations i = ',i
write(*,*)'Vm ideal = ',Vmideal
write(*,*)'Vm true = ',Vmnew
write(*,*)'Electrode spacing is ',d,' mm'
write(*,*)'The null current is ',current,' +/- ',currerror,' mA'
write(*,*)'The water Faraday cell calibration constant is ',Fcellcalib,'rad/mA'
write(*,*)'The electric field is ',Ex
write(*,*)'The cell pressure is ',P,' Pa'
write(*,*)'The voltage applied to the cell is ',voltage,' V'
write(*,*)'The room temperature is ',temp,' K ',(temp-273.15),' deg C'
write(*,*)'Aepsilon is ',ae
write(*,*)'Bepsilon is ',ae*b
write(*,*)'The epsilon_r value is ',er
```

```
write(*,*)'The refractive index is ',n


write(10,*)'Helium run'
write(10,*)' '
write(10,*)'Vm iterations i = ',i
write(10,*)'Vm ideal = ',Vmideal
write(10,*)'Vm true = ',Vmnew
write(10,*)'Electrode spacing is ',d,' mm'
write(10,*)'The null current is ',current,' +/- ',currerror,' mA'
write(10,*)'The water Faraday cell calibration constant is ',Fcellcalib,'rad/mA'
write(10,*)'The electric field is ',Ex
write(10,*)'The cell pressure is ',P,' Pa'
write(10,*)'The voltage applied to the cell is ',voltage,' V'
write(10,*)'The room temperature is ',temp,' K ',(temp-273.15),' deg C'
write(10,*)'Gamma_K ',GAMMA_K!,' +/- ',mQ*currerror/current,' C m^5 J^-1 mol^-1'
write(10,*)'Aepsilon is ',ae
write(10,*)'Bepsilon is ',ae*b
write(10,*)'The epsilon_r value is ',er
write(10,*)'The refractive index is ',n
close(10)
End Program
```